Mississippi State University
Scholars Junction

Theses and Dissertations | Theses and Dissertations

5-1-2009

Use of high resolution microscopy (FESEM and TEM) to investigate carbonate precipitates in association with organic matter from hot spring, salt pond, and reef environments

Margaret Elizabeth Corley

Follow this and additional works at: https://scholarsjunction.msstate.edu/td

Recommended Citation
Corley, Margaret Elizabeth, "Use of high resolution microscopy (FESEM and TEM) to investigate carbonate precipitates in association with organic matter from hot spring, salt pond, and reef environments" (2009). *Theses and Dissertations*. 4868.
https://scholarsjunction.msstate.edu/td/4868

This Graduate Thesis - Open Access is brought to you for free and open access by the Theses and Dissertations at Scholars Junction. It has been accepted for inclusion in Theses and Dissertations by an authorized administrator of Scholars Junction. For more information, please contact scholcomm@msstate.libanswers.com.

www.manaraa.com

USE OF HIGH RESOLUTION MICROSCOPY (FESEM AND TEM) TO INVESTIGATE CARBONATE PRECIPITATES IN ASSOCIATION WITH ORGANIC MATTER FROM HOT SPRING, SALT POND, AND REEF ENVIRONMENTS

By

Margaret Elizabeth Corley

A Thesis
Submitted to the Faculty of
Mississippi State University
in Partial Fulfillment of the Requirements
for the Degree of Master of Science
in Geology
in the Department of Geosciences

Mississippi State, Mississippi

August 2009

www.manaraa.com

USE OF HIGH RESOLUTION MICROSCOPY (FESEM AND TEM) TO INVESTIGATE CARBONATE PRECIPITATES IN ASSOCIATION WITH ORGANIC MATTER FROM HOT SPRING, SALT POND, AND REEF ENVIRONMENTS

By

Margaret Elizabeth Corley

Approved:

Brenda L. Kirkland Assistant Professor of Geosciences (Director of Thesis)	Giselle Thibaudeau Associate Professor (Committee Member)
Chris P. Dewey Associate Professor (Committee Member)	Gary L. Myers Dean of College of Arts and Sciences

www.manaraa.com

Name: Margaret Elizabeth Corley

Date of Degree: August, 2009

Institution: Mississippi State University

Major Field: Geology

Major Professor: Dr. Brenda L. Kirkland

Title of Study: USE OF HIGH RESOLUTION MICROSCOPY (FESEM AND TEM) TO INVESTIGATE CARBONATE PRECIPITATES IN ASSOCIATION WITH ORGANIC MATTER FROM HOT SPRING, SALT POND, AND REEF ENVIRONMENTS

Pages in Study: 54

Candidate for Degree of Master of Science

Carbonate precipitates in biofilm were investigated from hot springs near Viterbo, Italy; Salt Pond, San Salvador, and Fowl Cay Reef, Abaco, The Bahamas. Features shared by hot springs and salt ponds are supersaturation with $CaCO_3$, abundant *Spirulina*, and clustered acicular aragonite crystals termed "fuzzy dumbbells." TEM and FESEM microscopy show fuzzy dumbbells contain cores of amorphous organic matter and subhedral $CaCO_3$ microcrystals arranged in linear fabrics. Micron- to millimeter-scale microenvironments are identified by localized dissolution, the occurrence of gothic calcite inter-grown with organic filaments, and the presence of calcite in biofilm where aragonite is chemically favored. Spherical $CaCO_3$ precipitates in reefs were anticipated, but not encountered in TEM sections of reef biofilm. In conclusion, biofilm creates the microenvironment and organic matter provides substrate for fuzzy dumbbell precipitation. TEM is a novel technique for studying the relationship between organic matter and $CaCO_3$ precipitation, and has potential medical, industrial, and academic applications.

www.manaraa.com

DEDICATION

This work is dedicated to my grandfather, Horace Corley, who first taught me to reason, to Leo Lynch, who crystallized my love of geology, and to my youngest brother Thomas Jones, who loved me no matter what.

www.manaraa.com

ACKNOWLEDGEMENTS

While the nature of microscopy work is hours spent on one's own in front of a scope, this thesis was by no means accomplished alone.

Many thanks to Dr. Robert L. Folk, his close investigation of life is the foundation this work stands on.

I am grateful to Dr. Brenda Kirkland for advice, supervision, editing, sometimes food, and all the little things that fall between.

I appreciate the constructive comments and time spent on my thesis by my committee members, Giselle Thibaudeau and Dr. Chris Dewey. Dr. Dewey has been an invaluable mentor for the past six years, it is impossible to list here how much better I am for it.

The beautiful formatting of this document is entirely due to Thomas La Foe and James Nail, both close friends and library experts.

I also benefited from the patient assistance of Richard Kuklinski, Bill Monroe and especially Amanda Lawrence at the MSU EM Center. This work could not have been done without Amanda, who is an amazing scientist and an even more amazing friend.

I can never give enough thanks to my mother, Margaret Tyer. Her constant support throughout my life has enabled me to do whatever I want and succeed.

Thanks also to my brother Wilson Jones, for never taking me too seriously; and the rest of my family for their loving support.

www.manaraa.com

I must thank my teachers and my department. Without the MSU Geosciences family I could not have come this far, especially this last semester. It is amazing that you are too many to name, but you know who you are. I am grateful of the opportunities you pushed me to try for, the flaws you helped correct, the knowledge (and incredibly hard homeworks) you gave, and the support I received. You have kept me whole.

Dr. W.W.Wilson first saw in me an ability for science. He was an invaluable mentor in my undergraduate career, allowing me to learn the precision and dedication necessary for research while in his lab. His early help enabled me to appreciate the focus needed for good science, and the rewards that come from it. I am continually inspired by his example.

Last but not least, I thank Tony Morris, who has rescued me from a lot of small crises, cooked a lot of dinners, done a lot of shopping, and made me take needed breaks. It is impossible to thank him enough.

www.manaraa.com

TABLE OF CONTENTS

Page

DEDICATION ii

ACKNOWLEDGEMENTS iii

LIST OF FIGURES vii

CHAPTER

I. INTRODUCTION 1

Background 2
Significance 3

II. METHODS 4

Sample Acquisition 4
Hot Springs 4
Salt Pond 4
Reef 5
Sample Preparation 5
Scanning Electron Microscopy 5
Transmission Electron Microscopy 6
Confocal Microscopy 7
Environmental Electron Microscopy 8

III. RESULTS 9

Scanning Electron Microscopy 9
Hot Spring Sample 08A 9
Hot Spring Sample 08B 13
Hot Spring Sample 08C 19
Hot Spring Sample 08D 25
Transmission Electron Microscopy 30
Salt Pond Samples 30
Reef Samples 37
Other Approaches 41

www.manaraa.com

IV. DISCUSSION 43

V. CONCLUSIONS 50

REFERENCES 52

www.manaraa.com

LIST OF FIGURES

FIGURE Page

1 Gothic calcite from Bullicame Dante Spring, Viterbo, Italy. A: "shingling sheet" morphology; B: a ~1 μm diameter mucilagenous sheath; C: <10 nm diameter filaments 10

2 Calcite in a filament network from Bullicame Dante Spring, Viterbo, Italy A: An enclosed organic filament; B: Channel made by calcite partially enclosing a filament; C: Empty channel that shows growth bands; D: A mucilage lined tube through calcite. E: <10nm diameter filaments F: An unknown small helix. 11

3 Filaments and microbes on calcite from Bullicame Dante Spring, Viterbo, Italy. A: Channel made by calcite partially enclosing a filament; B: Empty channel which shows growth bands; C: A Mucilage lined tube through the crystal; D ~1 μm long ovoid; E: ~0.3 μm/ ~300 nm in diameter ovoid-shaped microbes; F: Nanometer scale spheroids; G: An unknown small helix.....12

4 Calcite from Bullicame Dante Spring, Viterbo, Italy. A: Channel made by calcite partially enclosing a filament showing growth bands; B: ~1 μm long ovoid; C: ~0.3 μm/ ~300nm in diameter ovoid-shaped microbes; D: An unknown small helix showing the characteristic "shepherd's crook".....13

5 Calcite from Bullicame Piccolo Springs, Viterbo, Italy and surrounding filament network. A: Channel made by calcite partially enclosing a filament showing growth bands; B: Tube through calcite with remnant mucilagenous sheath; C: ~1 μm and ~0.3 μm microbes 15

6 Calcite from Bullicame Piccolo Springs, Viterbo, Italy and "shepherd's crook".....16

7 Calcite from Bullicame Piccolo Springs, Viterbo, Italy. Aragonite is present in the filamentous mass indicated by the red box. The area in the red box is shown in higher magnification in Figure 8 17

www.manaraa.com

FIGURE Page

8 Aragonite in biofilm from Bullicame Piccolo Springs, Viterbo, Italy. A: Acicular aragonite crystal with relatively small needles; B: Acicular aragonite crystals with larger needles; C: Dolomite shaped rhomb 18

9 Bullicame Piccolo Springs, Viterbo, Italy. A: Dolomite-shaped rhomb that has not completely formed; B: Acicular aragonite with rounded crystal termini 19

10 Gothic calcite and biofilm from Bullicame Dante Spring, Viterbo, Italy. Calcite in this sample shows trigonal symmetry. A: ~1µm elongate ovoid microbes; B: ~0.3µm ovoid microbes 21

11 Calcite and biofilm from Bullicame Dante Spring, Viterbo, Italy. A: Calcite with trigonal symmetry; B: Channel in calcite left by a partially enclosed filament; C: ~1µm elongate ovoid microbes; D: "chains" of deflated, ovoid cells 22

12 Calcite from Bullicame Dante Spring, Viterbo, Italy, showing trigonal symmetry 23

13 Acicular aragonite in the form of a "fuzzy dumbbell" from Bullicame Dante Spring, Viterbo, Italy. A: Organic filaments and rod-shaped bacteria overlying aragonite crystals; B: Rounded termini of acicular aragonite crystals 24

14 Bottom portion of aragonite fuzzy dumbbell in Figure 13. A: ~10 nm filament overlaying aragonite crystals; B: Rounded termini of acicular aragonite crystals 25

15 Acicular aragonite fuzzy dumbbells and associated microbes from Le Zitelle Springs, Viterbo, Italy. 1A: Spirulina; B: Rod-shaped microbes; 2A: Pitted aragonite crystals due to dissolution; B: Aragonite crystals free from dissolutional features; 3A: Amorphous ovoids within core; B: Pitted aragonite crystals at exterior; 4A: ~0.3 µm microbes on fuzzy dumbbell surface 27

16 1: Surface features of Spirulina; 2A: Dissolution of acicular aragonite; B: Acicular aragonite precipitating on Spirulina. 28

www.manaraa.com

FIGURE Page

17 1A: Sub-micron filaments and sub-micron spheres on aragonitic fuzzy dumbbell; 2A: Amorphous heterogeneous core showing radial linear fabric; B: ~200 nm transition zone composed of elongate ovoids; 3A: Rounded terminus of broken aragonite crystal; 4: Similar features to those found in fuzzy dumbbells present within botryoidal acicular aragonite precipitate....29

18 TEM images of an aragonitic fuzzy dumbbell in cross section. 1: 5000x image of entire dumbbell; 2: 20,000x image of fuzzy end of dumbbell; 3: 67,000x image of transition zone between organic and inorganic zones in "fuzzy" end of dumbbell; 4: 67,000x image of transition zone in "bar" region of dumbbell....31

19 Aragonitic fuzzy dumbbell from Salt Pond, San Salvador, The Bahamas. Figure 20 shows areas of this dumbbell in greater detail....33

20 Details from Figure 19 at much higher resolutions. 1: 10,000x magnification of fuzzy end of dumbbell and ~200 nm transition zone. Radial linear features can be distinguished; 2: 100,000x magnification of ~200 nm transition zone; 3: 100,000x magnification of amorphous interior; 4: 140,000x magnifications – the maximum possible for the TEM at the MSU Electron Microscope Center in 2009....34

21 Aragonitic fuzzy dumbbell from Salt Pond, San Salvador, The Bahamas....35

22 Aragonitic fuzzy dumbbell from Le Zitelle Springs, Viterbo, Italy. Photomicrograph by Dr. B.L. Kirkland....36

23 1: 8000x image of aragonitic fuzzy dumbbell from Salt Pond, San Salvador, The Bahamas, with typical associated Spirulina; 2: 20,000x image of a cross section through Spirulina....37

24 A typical fabric in reef biofilm from Fowl Cay Reef, Abaco, The Bahamas....39

25 An unidentified cell common in biofilms from Fowl Cay Reef, Abaco, The Bahamas....40

26 Crystal growth within a cell commonly found in biofilms from Fowl Cay Reef, Abaco, The Bahamas....40

www.manaraa.com

FIGURE Page

27 1: shows a collection of elongate ovoid precipitates, ~1-2 μ m in length. 2: At 20,000x the slight dumbbell shape is more clearly seen. These precipitates do not have the same core features as aragonitic fuzzy dumbbells and are interpreted as artifacts of the staining process. 41

28 Equine serum albumin (a protein) crystals at 57X magnification grown from a supersaturated ESA solution. 45

29 TEM image of biofilm from Le Zitelle Spring,Viterbo, Italy. A: Nannobacteria in linear fabric of biofilm; B: Incipient acicular aragonite, forming on amorphous core; C: Amorphous organic matter. Photomicrograph by Dr. B.L. Kirkland. 47

www.manaraa.com

CHAPTER I

INTRODUCTION

The objective of this study is to compare textures in microstructure of carbonates at high resolution from three different environments using TEM, FESEM, ESEM, and confocal microscopy. The $CaCO_3$ precipitates are from hot springs near Viterbo, Italy (4 samples); biofilms from Fowl Cay Reef, Abaco, The Bahamas (7 samples, 9 to 20 m deep); and gelatinous sediment biofilm from Salt Pond, San Salvador, The Bahamas (5 samples, 5 cm to 30 cm deep). The environments differ in temperature, location, and chemistry, and a myriad of other factors, yet produce similar morphologies of calcium carbonate in the initial phase of precipitation. In each of these environments, precipitation occurs in microenvironments within biofilms where organic matter provides an initiation point for inorganic crystal precipitation. The environments also share features such as supersaturation with respect to $CaCO_3$, presence of *Spirulina*, and clusters of acicular aragonite known as "fuzzy dumbbells" (Pursell, 1985; Chafetz and Buczynski, 1990) The hypothesis tested was that precipitate occurs within biofilms and initiates on organic matter. The primary conclusion was that similar microbes (i.e. *Spirulina*) living in geologically and chemically different environments create chemically similar microenvironments. It may be that the microenvironment within biofilms is the common link between the similar crystal morphologies, and that this specific microenvironment is required for these unique $CaCO_3$ crystals to form.

www.manaraa.com

Background

Microbes and biofilms (aggregations of microbes and extracellular organic compounds) are now known to play a significant role in formation of carbonate rocks (Riding 2000). Although microbes in Bahamian tidal flats and ponds were noted long ago (Black, 1933, Shinn et al., 1969), the fields of geomicrobiology and now microbiogeochemistry have only evolved as a relatively new disciplines in geosciences over the last 15 years. The complexity of various microenvironments, millimeter-scale microbial communities, and zones of $CaCO_3$ precipitation in tidal flats is now being described in detail (Dupraz and Vissicher, 2005). Bacteria in algal mats clearly play a role in precipitation of dolomite (Vasconcelos and McKenzie, 1997) and nannobacteria-like particles have now been described from similar precipitates formed in the laboratory (Bontognali et al., 2008). The presence of bacteria within marine peloidal cements from reefs (Chafetz, 1986) and the role of biofilms in precipitation of microbialite in reef deposits is also well documented (Flugel, et al., 1993; Reitner, 1993; Zankl, 1993; Kirkland et al., 1998; Riding 2000). Bacteria were first documented in hot spring travertine deposits from central Italy (Chafetz and Folk, 1984). These hot springs also contain nannobacteria, which have been the focus of much debate (Nealson, 1997; Knoll and Osborn, 1999), including being implicated in the precipitation of calcium carbonate (Folk, 1994) and cited as evidence of very old life on Mars (McKay et al., 1996; McKay et al., 1997).

www.manaraa.com

Significance

This thesis documents the first TEM images of fuzzy dumbbells (R.L. Folk, personal communication to B.L. Kirkland, October 8, 2008). Development of our TEM technique represents a novel approach to the search for the relationship between organic matter and carbonate cement. The concept that initial precipitation of $CaCO_3$ crystals occurs within biofilm and originates from the exteriors of "nannobacteria-like" particles or extracellular polymeric substances (Bontognali et al., 2008) has implications in other fields, for example arterial calcification (Miller et al., 2004), calcium deposition in the placenta by a nannobacteria-like infection (Agababov, et al., 2007), and kidney stone production (Kajander and Çiftçioglu, 1999). In industrial settings, precipitation of $CaCO_3$ within biofilms may influence formation of pipe scale. In the petroleum industry secondary recovery efforts involving bacteria might also result in crystal precipitation. This thesis documents potentially analogous nanometer-scale precipitates in natural environments and innovative describes analytical techniques applicable to other disciplines.

www.manaraa.com

CHAPTER II

METHODS

Sample Acquisition

Hot Springs

Samples were collected on May 14, 2008 from hot springs near Viterbo, Italy, ~80 km northwest of Rome by Dr. Robert L. Folk with assistance from J. Horowitz and Deanna Combs. Sample 08A was collected from the outflow of Bullicame Dante Spring. Samples 08B and 08C were collected from the stream at Bullicame Piccolo Springs, and sample 08 D from Le Zitelle Springs just outside a fence surrounding the springs (Schematic of study area is found in Appendix A).

Samples were sealed in plastic containers and shipped to Mississippi State University in two water-proof bags (hygienic and air sickness bags) one inside the other.

Salt Pond

Samples were collected from Salt Pond, San Salvador, The Bahamas, by Keith Puckett with assistance from Dr. Karen McNeal. Salt Pond is a hypersaline inland pond with an area of approximately 0.05 km^2 separated from the ocean by a dune ridge. The pond waters come primarily from precipitation, seepage, and storm overwash. Samples were taken in the dry season from push cores along the third permanent transect of the

www.manaraa.com

pond at distances of 0, 11, 17, 23, and 50 m from the start of the transect. The water level of the pond at this time was at the 17 m mark; following the rainy season, water had risen to the 6 m mark. Samples were preserved in a 1.5% v/v (volume per volume) glutaraldehyde solution on site and shipped back to MSU for analysis.

Reef

Samples were collected by Keith Puckett from Fowl Cay Reef, Abaco, The Bahamas in an area known locally as "Grouper Alley". Wave base in this area is about 9 m. Samples were collected at a range of depths (4.5 to 20 m) and conditions (sunlight, wave activity, substrate type) by SCUBA divers and placed in Nalgene bottles with seawater. At the surface, glutaraldehyde was added to a concentration of ~1.5% v/v.

Sample Preparation

Scanning Electron Microscopy

Scanning electron microscopy (FESEM, model JEOL JSM-6500F) was used to create high-magnification images of sample surfaces. The reef and salt pond samples, initially preserved in 1.5% v/v glutaraldehyde in sea-water solution, were prepared for SEM analysis at the Electron Microscopy Center at MSU. All of the samples, including those from the hot springs were osmicated, then chemically dehydrated using the protocol of a minimum of 2 hr in 2.5% glutaraldehyde in 0.1 M potassium phosphate buffer, 10 min each in 35%, 50%, 70% and 95% ethanol, 6 x 10 min changes of 100% ethanol, and finally hexamethyldisilazane (HMDS) for 10 min after which the sample was allowed to

www.manaraa.com

air dry. Samples were mounted to aluminum stubs using either hot glue or carbon tape, depending on sample shape. Once mounted, stubs and samples are coated for 60 sec with Au/Pd in a sputter coater, yielding a coating of 15 nm.

The hot spring calcium carbonate precipitates collected by B.L. Kirkland in 1998 from La Zitelle Springs, Viterbo, Italy, were calcium carbonate precipitates, and did not require dehydration. These samples were carefully fractured to expose fresh, broken surfaces, and were then mounted and coated as described above.

Transmission Electron Microscopy

Transmission Electron Microscopy (TEM model JEOL JEM-100CXII) was used to produce high-resolution images of samples, including precipitates, biofilm, and biofilm components. TEM was used to analyze hot spring, reef, and salt pond samples. Images on samples were compared to TEM images of the hot spring samples made previously by Dr. B. L. Kirkland's research group.

Samples were preserved in the field as listed above, and then brought to MSU to be prepared for TEM. The samples were first rinsed with salt water, osmicated, rinsed again, and then dehydrated chemically using the protocol of 2 hrs in 2.5% glutaraldehyde in 0.1 M potassium phosphate buffer, 10 min each in 35%, 50%, 70% and 95% ethanol followed by 6 x 10 minute changes of 100% ethanol. They were then rinsed, stained with osmium tetroxide, and infused with resin, using a progressive increase in Spurr's resin concentration: 25, 50, 75, and 100% (Spurr, 1969). Once samples were in 100% epoxy resin, they remained in resin for several days, with the resin being changed two times per

www.manaraa.com

day. Finally, the samples were placed in block molds and cured in a 68°C oven overnight.

Once blocks were completely cured, they were trimmed to expose the sample area and then were faced to prepare the block for cutting by an ultra-microtome (model Reichert Jung Ultracut E). The ultra-microtome cuts 0.1µm-thick sections to identify an area of interest. The sections were collected on a microscope slide, stained for 3 min with Toluidine Blue and for 30 sec with Safranin. They were then analyzed on both petrographic and confocal microscopes.

Once an area of interest was identified, the block was cut into 0.75 nm thin sections. The sections were collected on a copper grid, and allowed to dry. They were then stained with uranyl acetate for 20 min and with lead citrate for 5 min. A few sections were left unstained as a control, as staining may lead to precipitate formation on the section and grid. At this point, the samples were ready for analysis on the TEM.

Confocal Microscopy

Confocal microscopy (model ZEISS LSM-510) produced relatively low-magnification images of our samples. Using different wavelengths of light and different filters, we were able to distinguish a variety of materials in the sample by their auto-fluorescence. Paraffin sections, thick sections from the ultra microtome, and small fragments of dried samples mounted to microscope slides, were analyzed in this way.

Samples for the confocal were arranged on a microscope slide, covered by a cover slip and sealed with Permount. Some samples were unprocessed from the field and some were thoroughly processed from TEM blocks. All the samples were analyzed to

www.manaraa.com

determine the optimum set of wavelengths and filters for analysis. They were then scanned at maximum resolution at magnifications of 5, 10, 20, 40, 60, and 100x.

Environmental Electron Microscopy

Environmental Electron Microscopy (Zeiss EVO-40XVP) (ESEM) was used to examine samples from Salt Pond. Portions of samples were removed from fixative, rinsed, broken or cut into small (<5 x 5 mm fragments), mounted onto stubs, and placed into the chamber wet. Because dehydration is not required, the images taken with the ESEM were useful in determining that the dehydration process used for FESEM had not resulted in significant alteration of Salt Pond samples.

www.manaraa.com

CHAPTER III

RESULTS

Scanning Electron Microscopy

Hot Spring Sample 08A

The sample was collected 26 m from the outflow orifice of hot springs at Bullicame Dante Spring, Viterbo, Italy, from mostly unmineralized yellow green slime. Although collected at a temperature (~50°C) that would typically favor aragonite production (Folk, 1994) the sample contains primarily "gothic" calcite. The crystal is made of "shingling sheets" (Folk, personal communication, October 22, 2008) that overlap each other (Figure 1A).

Under higher magnification, thin (<10 nm in diameter) filaments are seen stretched across calcite crystals and attached to the large (~1 μm in diameter) filaments. The thin filaments, which are only visible on the calcite crystals, are still cylindrical as opposed to the sheaths of the larger filaments (Figures 1C, 2E, and 3H).

In this sample organic filaments typically ~1 to 2 μm in diameter are ubiquitous (Figure 1B). The filaments form a network that surrounds the calcite crystals (Figure 2). The crystals, in turn, enclose parts of the filaments (Figure 2A). Where removed by the dehydration process, the filaments leave channels (Figures 2B and 3A) in the calcite and reveal banding in the crystal (Figures 2C, 3B and 4A). The channels apparently result

www.manaraa.com

from the simultaneous growth of the filamentous microbes and the "shingling sheets" of the calcite crystal. The channels increase the porosity of the calcite crystals, albeit at a 1-2 µm level. Some filaments overgrown by the calcite crystals leave a tube that is sporadically either unlined or lined by the remnants of a mucilagenous sheath that remains in the crystal after dehydration (Figures 2D and 3C).

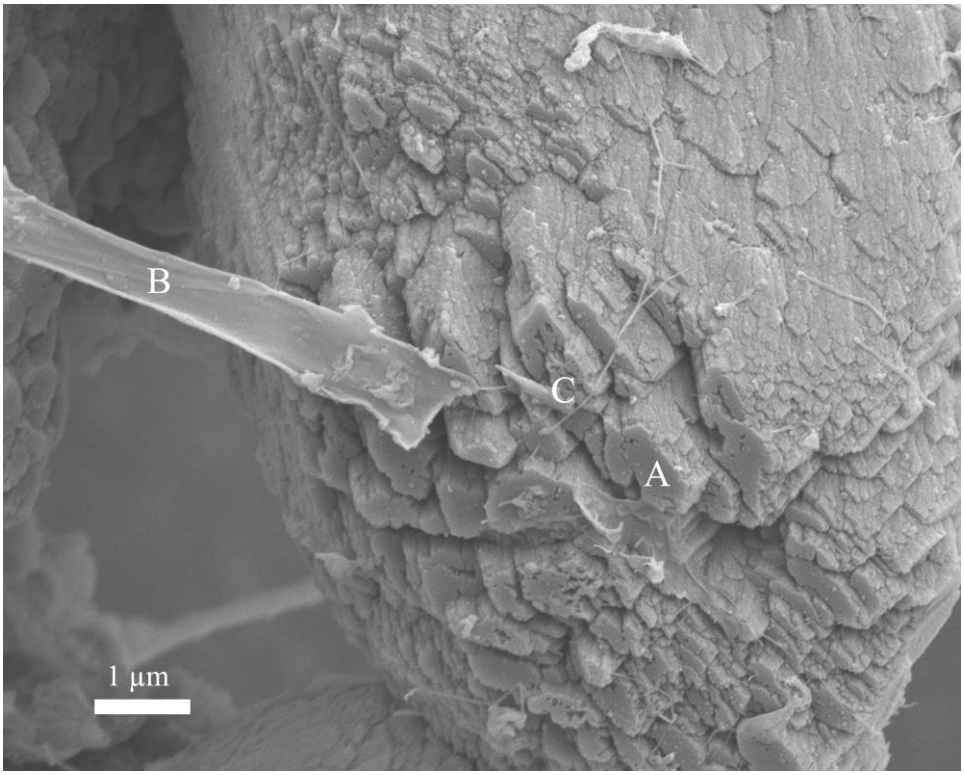

Figure 1 Gothic calcite from Bullicame Dante Spring, Viterbo, Italy. A: "shingling sheet" morphology; B: a ~1 µm diameter mucilagenous sheath; C: <10 nm diameter filaments

www.manaraa.com

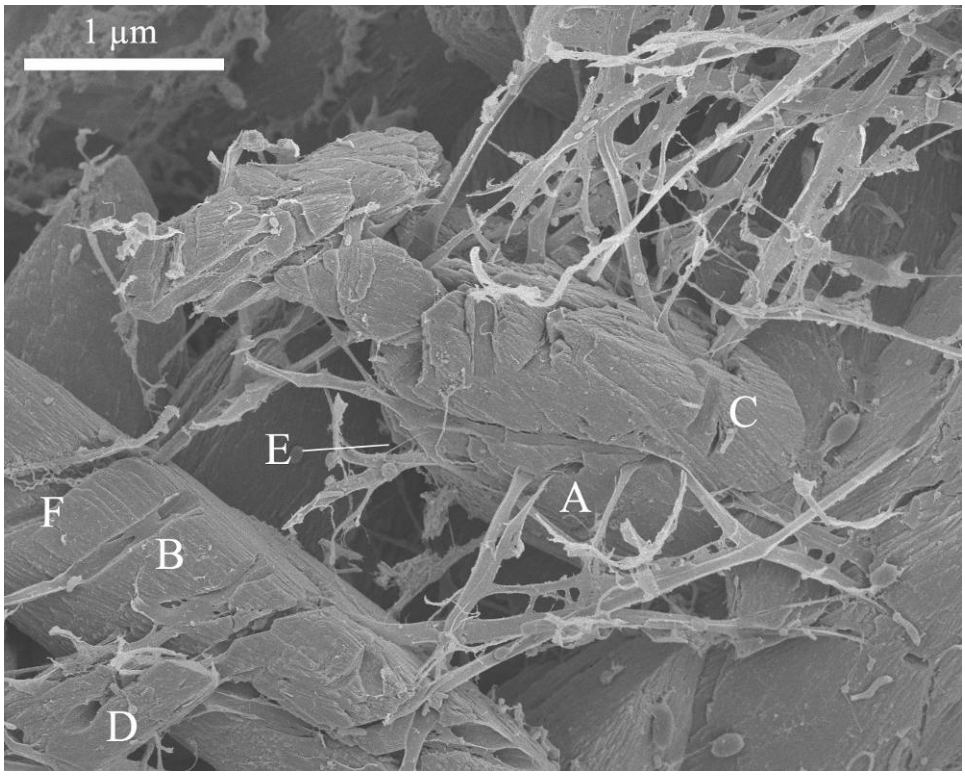

Figure 2 Calcite in a filament network from Bullicame Dante Spring, Viterbo, Italy. A: An enclosed organic filament; B: Channel made by calcite partially enclosing a filament; C: Empty channel that shows growth bands; D: A mucilage lined tube through calcite. E: <10nm diameter filaments F: An unknown small helix

Scattered on the filaments and crystal surface are slightly less than 1µm long ovoids (Figures 3D and 4B) and ~0.3 µm/ ~300 nm in diameter ovoid-shaped microbes (Figures 3E and 4C). Throughout the sample nanometer-scale spheroids are found on the surface of calcite crystals (Figure 3F). In addition, small (~120 nm in diameter), loosely coiled, helical microbes are common in the sample (Figures 2F, 3G, and 4D). They typically form a "shepherd's crook," identified as occurring at the growing end (Folk, personal communication). Through a light microscope, these helices are pale green.

www.manaraa.com

Unlike other organic filaments in this sample, the microbes have been deflated by dehydration.

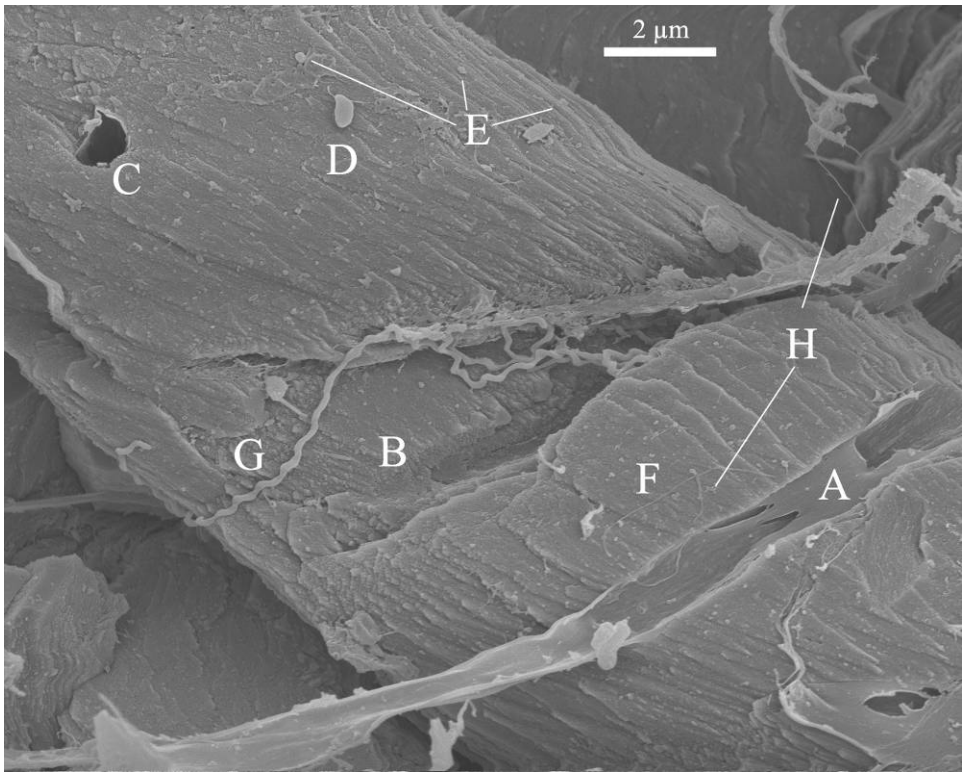

Figure 3 Filaments and microbes on calcite from Bullicame Dante Spring, Viterbo, Italy. A: Channel made by calcite partially enclosing a filament; B: Empty channel which shows growth bands; C: A Mucilage lined tube through the crystal; D ~1 µm long ovoid; E: ~0.3 µm/ ~300 nm in diameter ovoid-shaped microbes; F: Nanometer scale spheroids; G: An unknown small helix

www.manaraa.com

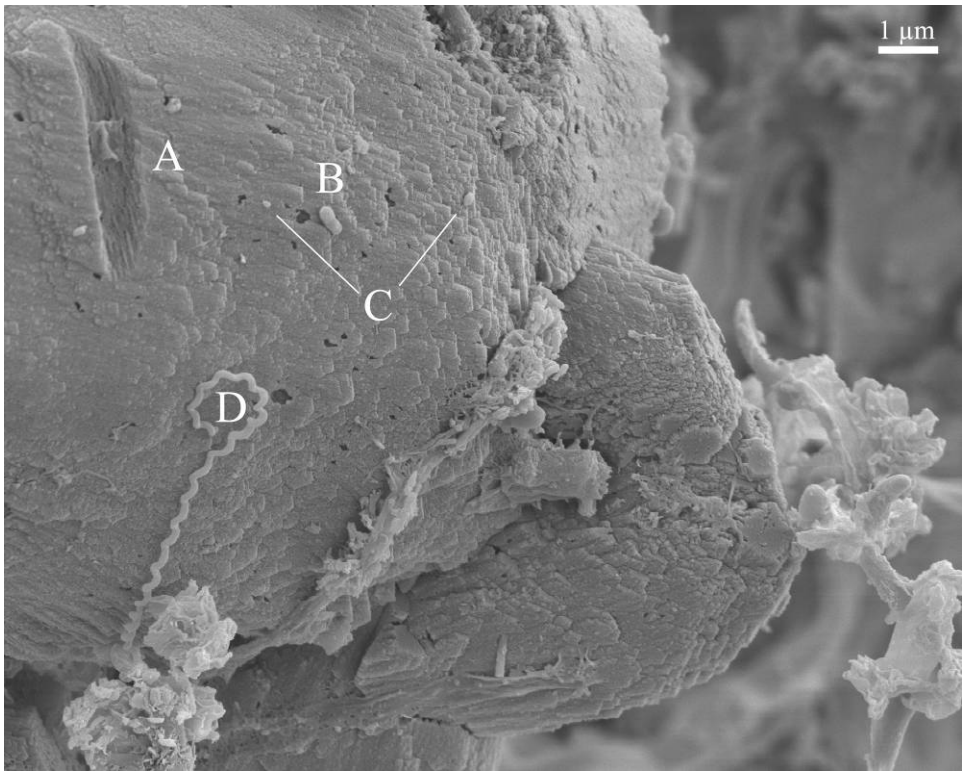

Figure 4 Calcite from Bullicame Dante Spring, Viterbo, Italy. A: Channel made by calcite partially enclosing a filament showing growth bands; B: ~1 µm long ovoid; C: ~0.3 µm/ ~300nm in diameter ovoid-shaped microbes; D: An unknown small helix showing the characteristic "shepherd's crook"

Hot Spring Sample 08B

The sample was collected from Bullicame Piccolo Springs, Viterbo, Italy where the spring water was 55 to 58°C. In contrast to other aragonite-dominated samples typical of springs in this temperature range (above 45°C), most of this sample is calcite. When collected the sample was dark green.

Organic filaments typically 1 to 2 µm in diameter are ubiquitous and resemble sheaths (Figure 5). The filaments form a network that surrounds the calcite crystals and the few aragonite crystals. The crystals in turn enclose parts of the filaments. Where removed by the dehydration process, the filaments leave channels in the calcite (Figure

www.manaraa.com

5A) that reveal banding similar to the crystals in sample 08A (Figures 1A, 2B, and 4A) . Again, this banding is apparently due to the simultaneous growth of the calcite crystal and the filamentous mat. These crystals also contain tubes left by removal of filaments and some tubes are still lined by remnant sheaths (Figure 5B).

As in sample 08A, the large (~1 μm in diameter) filaments and crystal surfaces bear occasional ovoid microbes of both ~1 μm and ~0.3 μm sizes (Figure 5C). Nanometer-scale spheroids (~100 nm) are scattered evenly on the surface of crystals. Very thin (<10 nm in diameter) filaments also occur. Light green, loosely coiled helical microbes (120 nm in diameter) are also present, again with a "shepherd's crook" at the growing end (Figure 6).

At higher magnification, small filaments (<10 nm in diameter) are found on calcite crystals and are attached to large (~1 micron) filaments. At higher magnification, smaller filaments occur on the surface of the calcite and are seen to stretch across calcite crystals as well as to attach to larger filaments.

www.manaraa.com

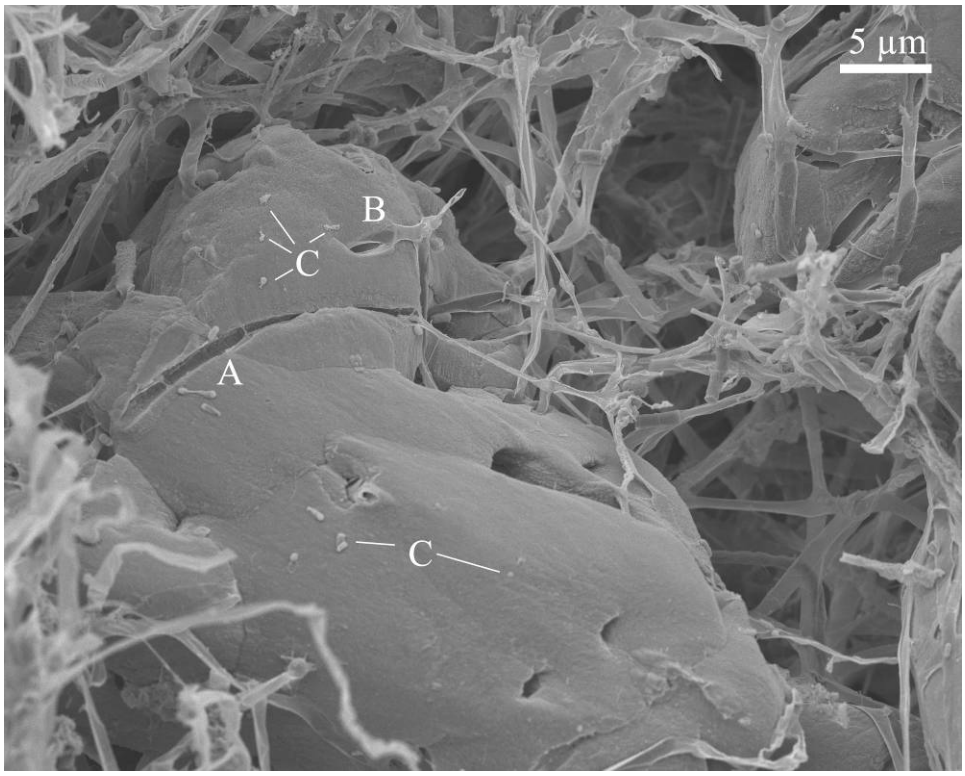

Figure 5 Calcite from Bullicame Piccolo Springs, Viterbo, Italy and surrounding filament network. A: Channel made by calcite partially enclosing a filament showing growth bands; B: Tube through calcite with remnant mucilagenous sheath; C: ~1 µm and ~0.3 µm microbes

www.manaraa.com

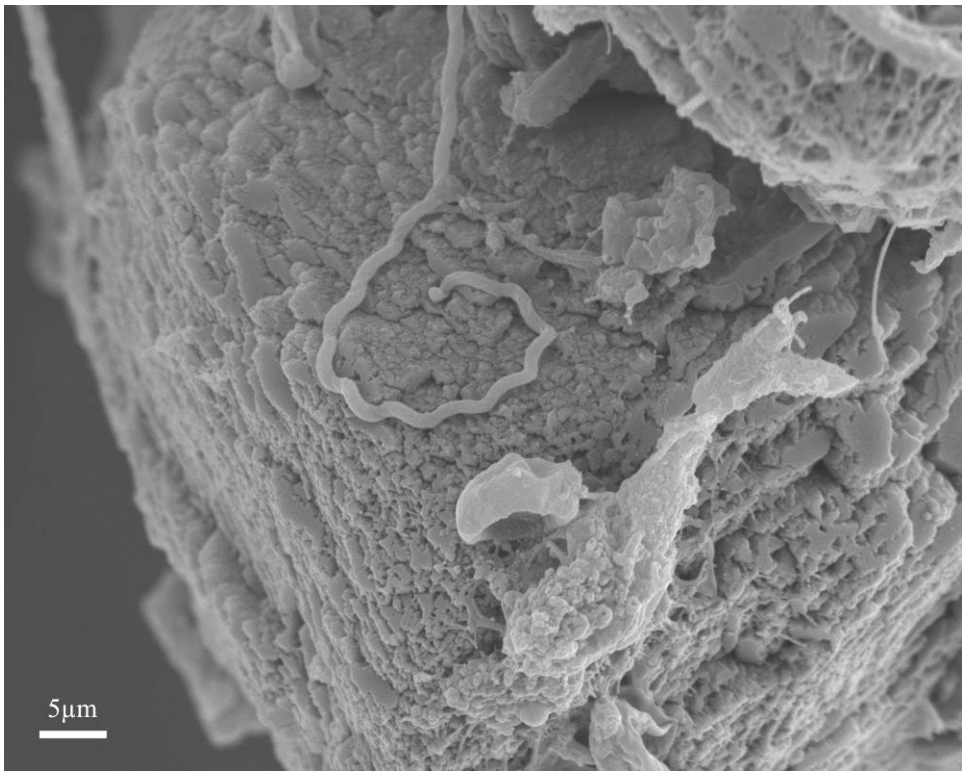

Figure 6 Calcite from Bullicame Piccolo Springs, Viterbo, Italy and "shepherd's crook"

In the areas of this sample where filaments are most dense, aragonite is present (Figure 7). The aragonite does not appear to grow around filaments as calcite does (Figures 7, 8, 9).

The three aragonite crystals in Figure 8 are the only three in this part of sample 08B. They occupy a small pocket within the filamentous mass. The large, spherical mass of crystals (Figure 8A) is composed of acicular aragonite crystals that are smaller than the acicular crystals of the two aragonite spheroids (Figure 8B) above it. To the right is a dolomite-shaped rhomb that has not completely formed (Figures 8C and 9). The termini of the aragonite needles when examined closely are spherical; not sharp or euhedral as might be expected (Figure 9).

www.manaraa.com

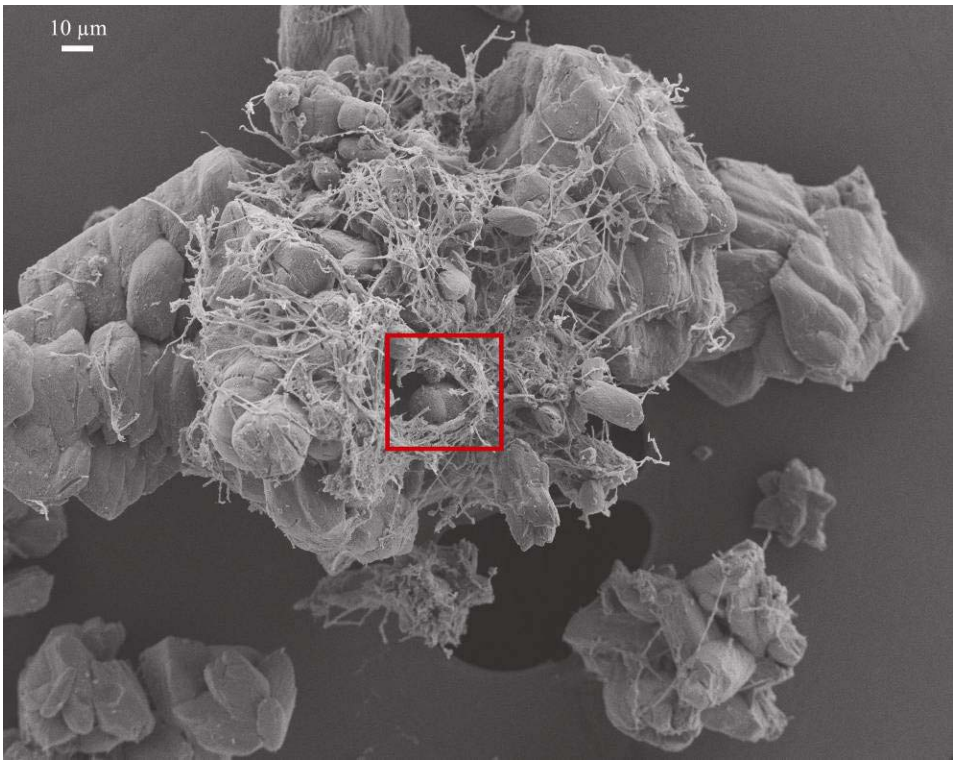

Figure 7 Calcite from Bullicame Piccolo Springs, Viterbo, Italy. Aragonite is present in the filamentous mass indicated by the red box. The area in the red box is shown in higher magnification in Figure 8.

www.manaraa.com

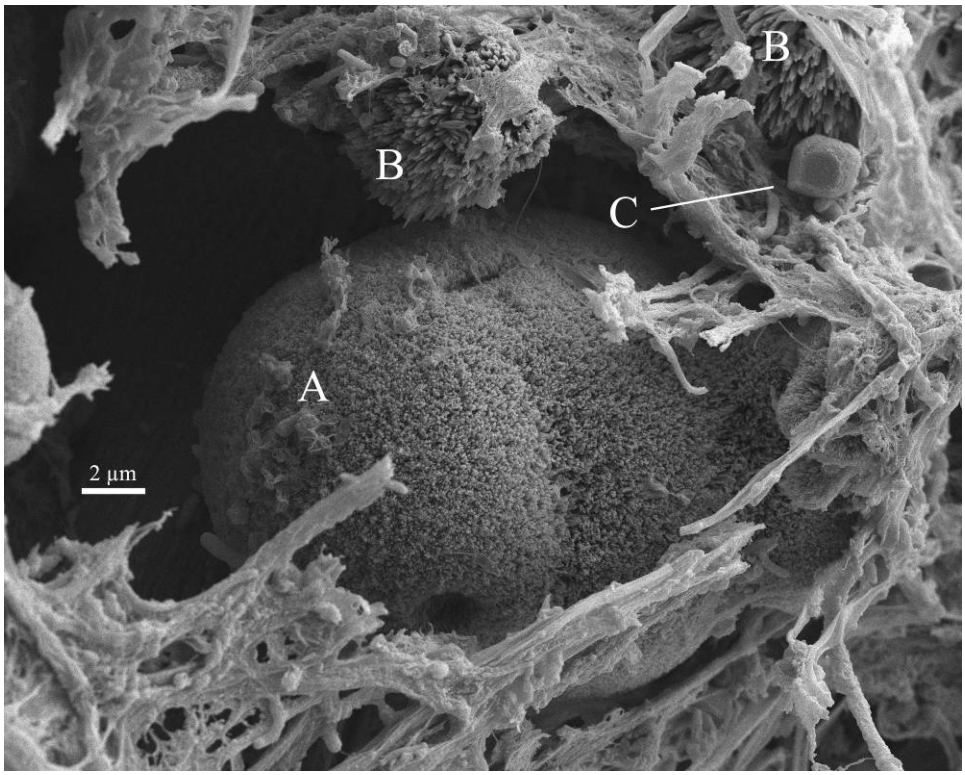

Figure 8 Aragonite in biofilm from Bullicame Piccolo Springs, Viterbo, Italy. A: Acicular aragonite crystal with relatively small needles; B: Acicular aragonite crystals with larger needles; C: Dolomite shaped rhomb

www.manaraa.com

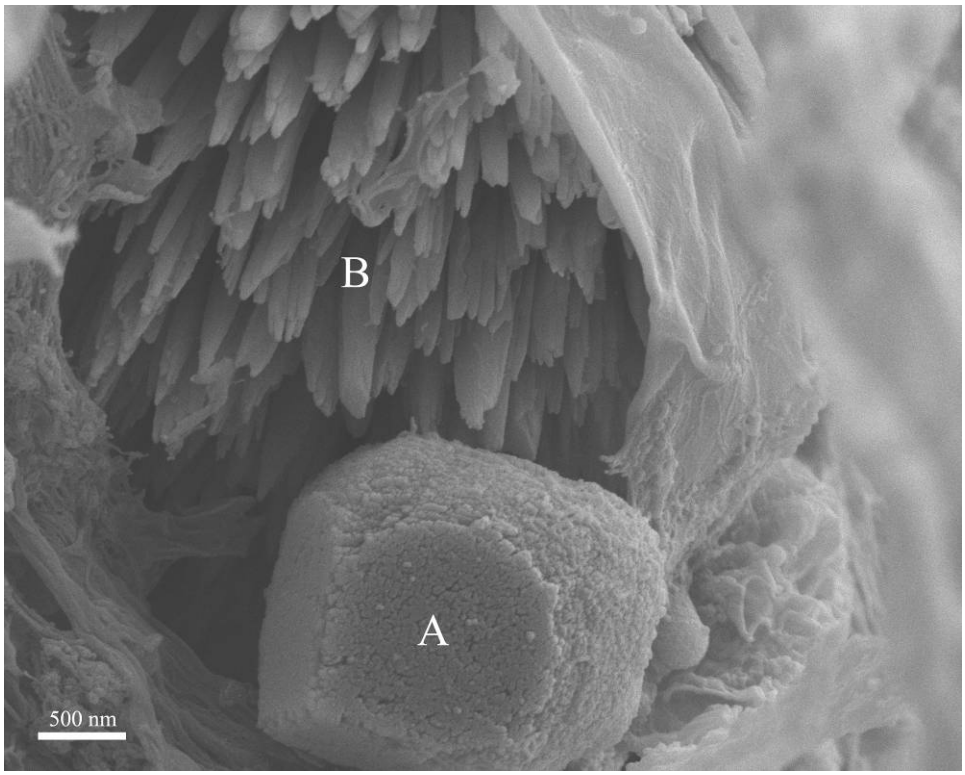

Figure 9 Bullicame Piccolo Springs, Viterbo, Italy. A: Dolomite-shaped rhomb that has not completely formed; B: Acicular aragonite with rounded crystal termini

Hot Spring Sample 08C

The sample was collected 8 m from the southern outflow of Bullicame Dante Spring, Viterbo, Italy. With the exception of a few aragonite crystals, minerals within this sample are calcite. The sample consisted of an orange slime collected from the flank of an overflow mound, in an area with high levels of elemental sulfur.

The sample contains organic filaments similar to those in samples 08A and 08B (Figures 2 and 5). In sample 08C the filaments form a much denser network (Figures 10 and 11). The calcite crystals have a "gothic" morphology exhibiting trigonal symmetry (Figures 11A and 12), and enclose parts of organic filaments (Figure 11). The dehydration procedure, as in the previous samples, resulted in formation of channels in

www.manaraa.com

the calcite crystals that have the same shape as filamentous microbes (Figure 11B). Where filaments are entirely removed, banding occurs in the calcite crystal as in samples 08A and 08B. Tubes through the crystals, some lined and some unlined by remnants of the mucilagenous sheath, occur where the filaments and crystals grew together synchronously.

As in samples 08A and 08B, ~1 μm filaments and calcium carbonate crystals are covered with a scattering of ovoid microbes ~1μm and ~0.3 μm and nanometer-scale spheroids (~100 nm in diameter) (Figures 10A, 10B and11C). Filaments less than ~10 nm in this sample are similar to those in samples 08A and 08B; however, in this sample, the helical, filamentous "shepherd's crook" seen in samples 08A and 08B is absent.

Figure 11D shows a "chain" of deflated, ovoid cells absent from the other hot spring samples. It also shows that this sample is the most complex and densely matted of the hot spring specimens. On the mat can be seen precipitate caught up in the network of filaments, a variety of microbes, and on every surface, a "dusting" of sub-micron spheres.

As with the aragonite in sample 08B, the crystal in sample 08C does not enclose filaments, instead the crystal is overlain by them (Figures 13A and 14A). This aragonite crystal is a "fuzzy dumbbell." Terminal ends of the aragonite needles are mostly rounded; only a few are euhedral (Figures 13B and 14B).

www.manaraa.com

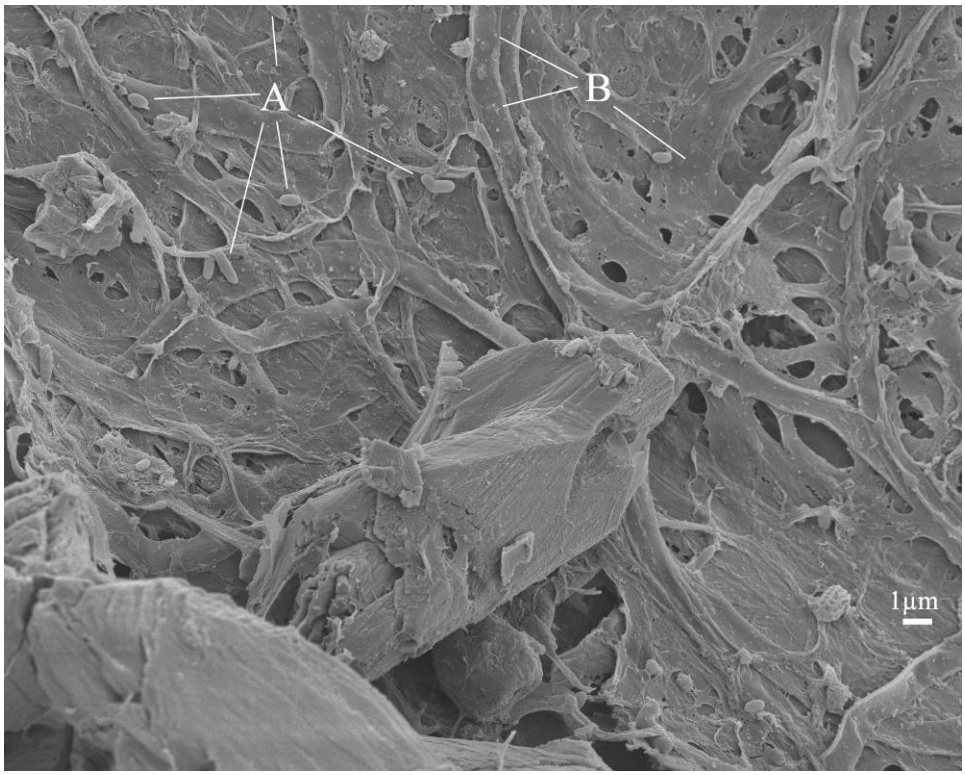

Figure 10 Gothic calcite and biofilm from Bullicame Dante Spring, Viterbo, Italy. Calcite in this sample shows trigonal symmetry. A: ~1µm elongate ovoid microbes; B: ~0.3µm ovoid microbes

www.manaraa.com

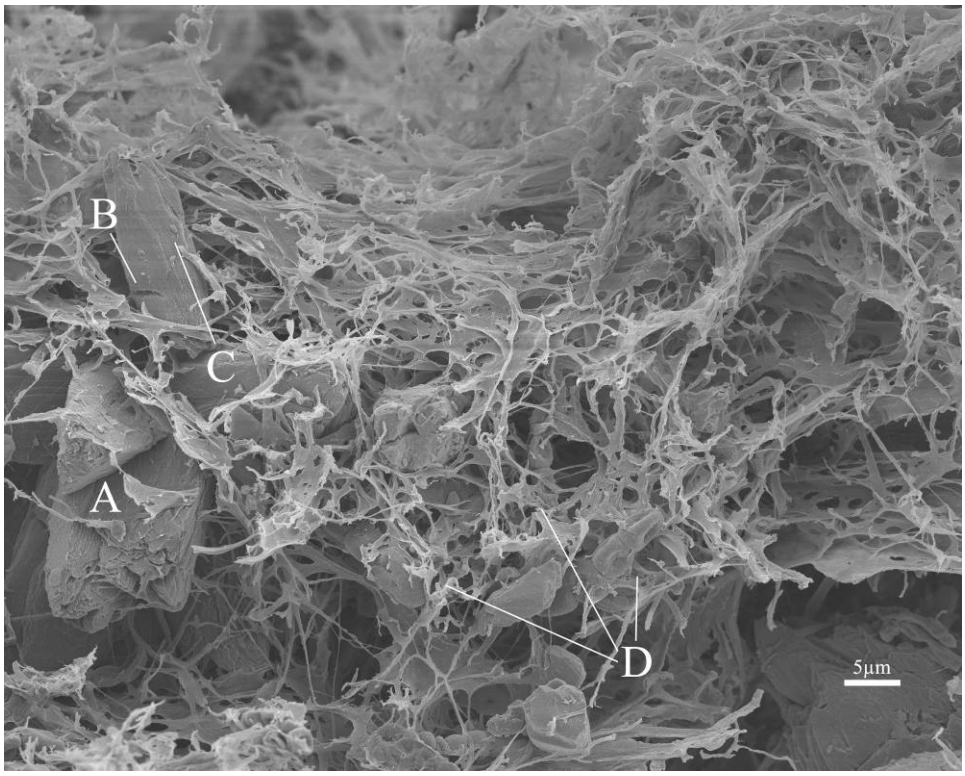

Figure 11 Calcite and biofilm from Bullicame Dante Spring, Viterbo, Italy. A: Calcite with trigonal symmetry; B: Channel in calcite left by a partially enclosed filament; C: ~1µm elongate ovoid microbes; D: "chains" of deflated, ovoid cells

www.manaraa.com

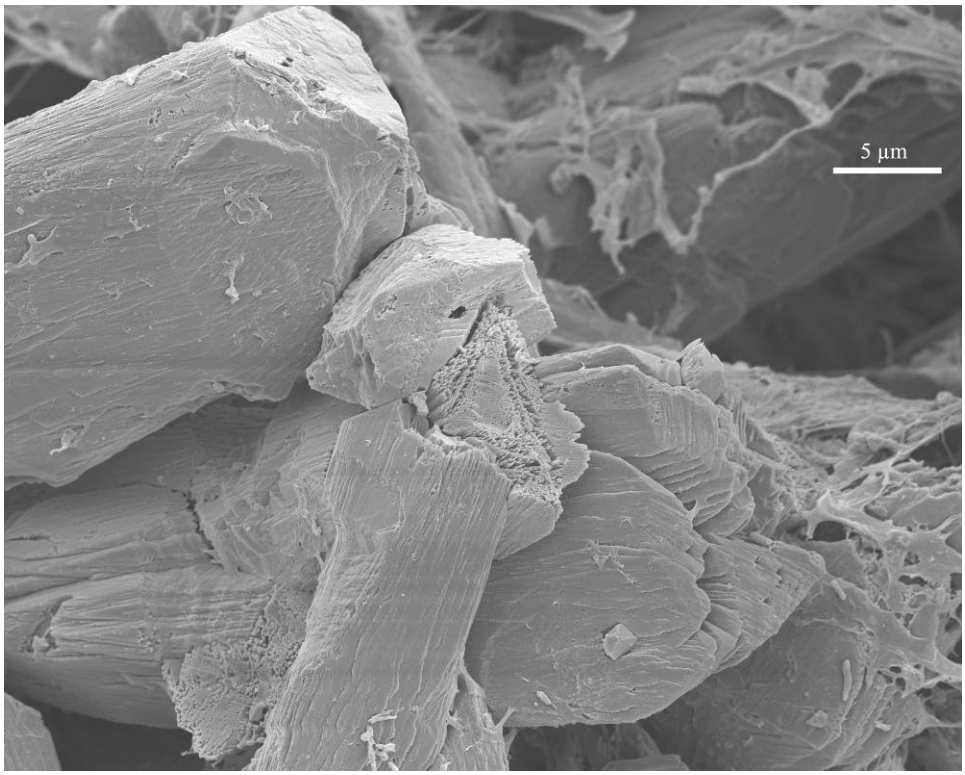

Figure 12 Calcite from Bullicame Dante Spring, Viterbo, Italy, showing trigonal symmetry.

www.manaraa.com

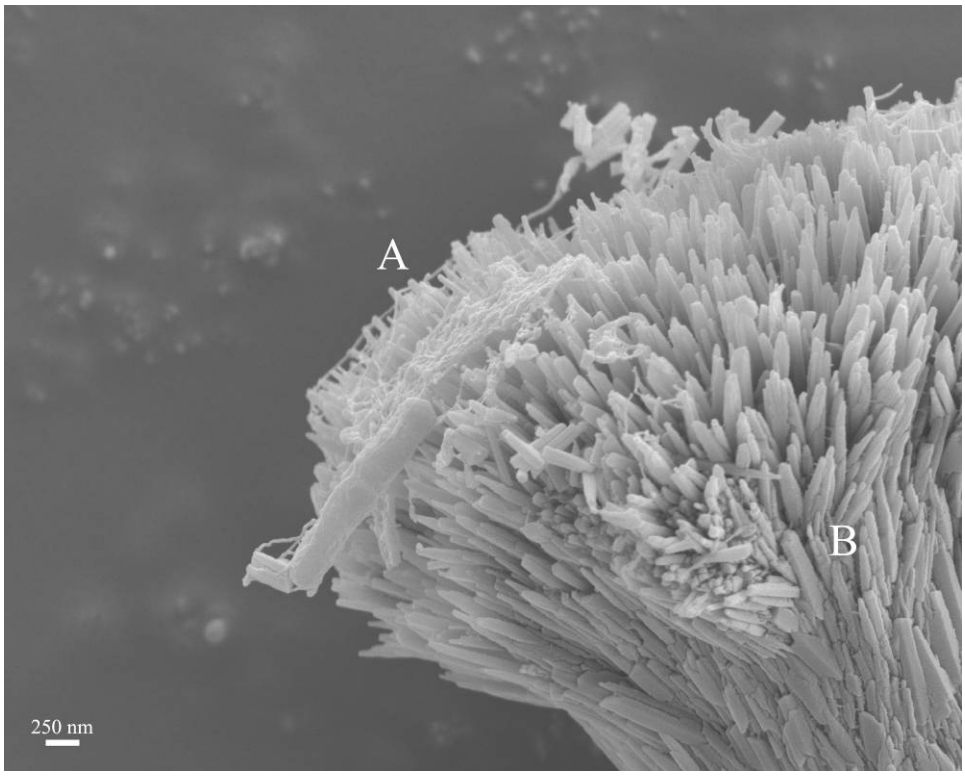

Figure 13 Acicular aragonite in the form of a "fuzzy dumbbell" from Bullicame Dante Spring, Viterbo, Italy. A: Organic filaments and rod-shaped bacteria overlying aragonite crystals; B: Rounded termini of acicular aragonite crystals

www.manaraa.com

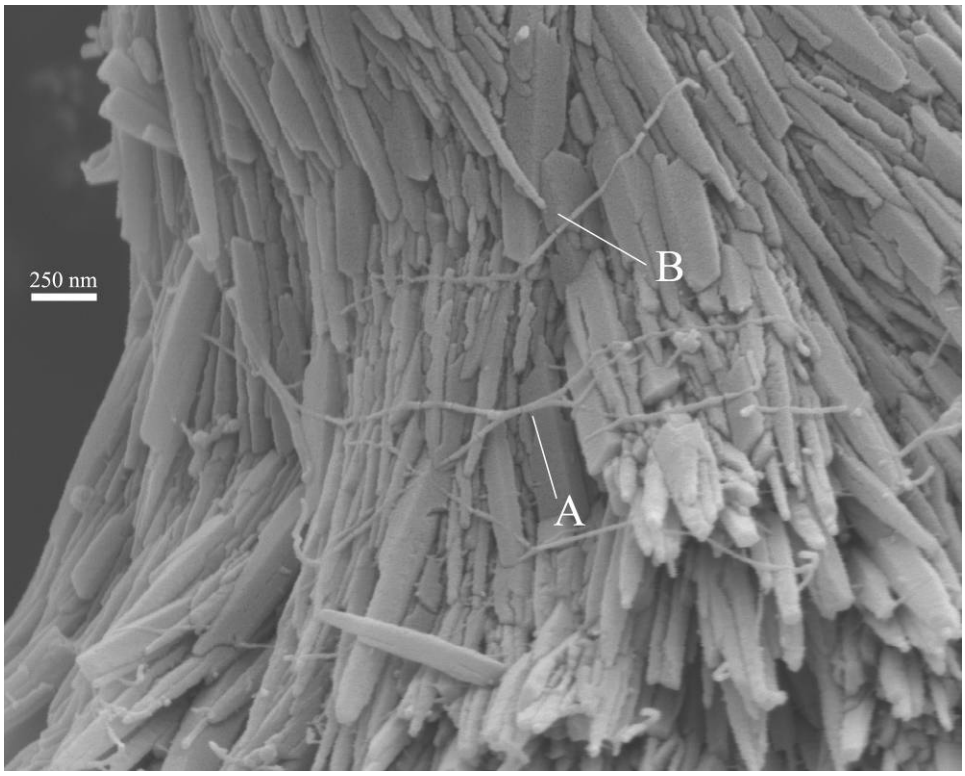

Figure 14 Bottom portion of aragonite fuzzy dumbbell in Figure 13. A: ~10 nm filament overlaying aragonite crystals; B: Rounded termini of acicular aragonite crystals

Hot Spring Sample 08D

The sample consists of one-centimeter tall gray, gelatinous "stalagmitic balls." The sample was obtained from at Le Zitelle Springs, Viterbo, Italy, from 45°C water (the coolest of springs sampled). Aragonitic rafts were forming at the surface. Calcite is absent. The predominant organism in this sample is *Spirulina* (Figure 15.1A), and rod-shaped bacteria are common (Figure 15.1B). Most aragonite in this sample consists of fuzzy dumbbells at various stages of formation and twinning. Close examination of needles that make up the fuzzy dumbbells reveals sub-micron filaments on their surface (Figure 15.4A).

www.manaraa.com

Figures15.2 and 15.3 show a dumbbell that was broken open before sample preparation. At high levels of magnification (11,000 and 50,000X) the core of the dumbbell is seen to be composed of amorphous spheres (15.3A). The spheres are variable in shape and size having a range of 15 to 40 nm (Figure 15.3). The surface of aragonite needles making up this broken dumbbell is pitted suggesting very localized dissolution (Figure 15.3B). The small spheres are concentrated in the center of the core, but are absent on its perimeter. Nearby acicular, euhedral aragonite needles do not show this pitting, and are unbroken (Figure 15.2A and Figure 15.2B)

Another broken dumbbell in this sample, mechanically broken during sample preparation, shows none of these features (Figure 15.4). In contrast to the previous example, there is no change in density of spheres from the center to the edge of the core, and there is no pitting on the surface of aragonite needles.

www.manaraa.com

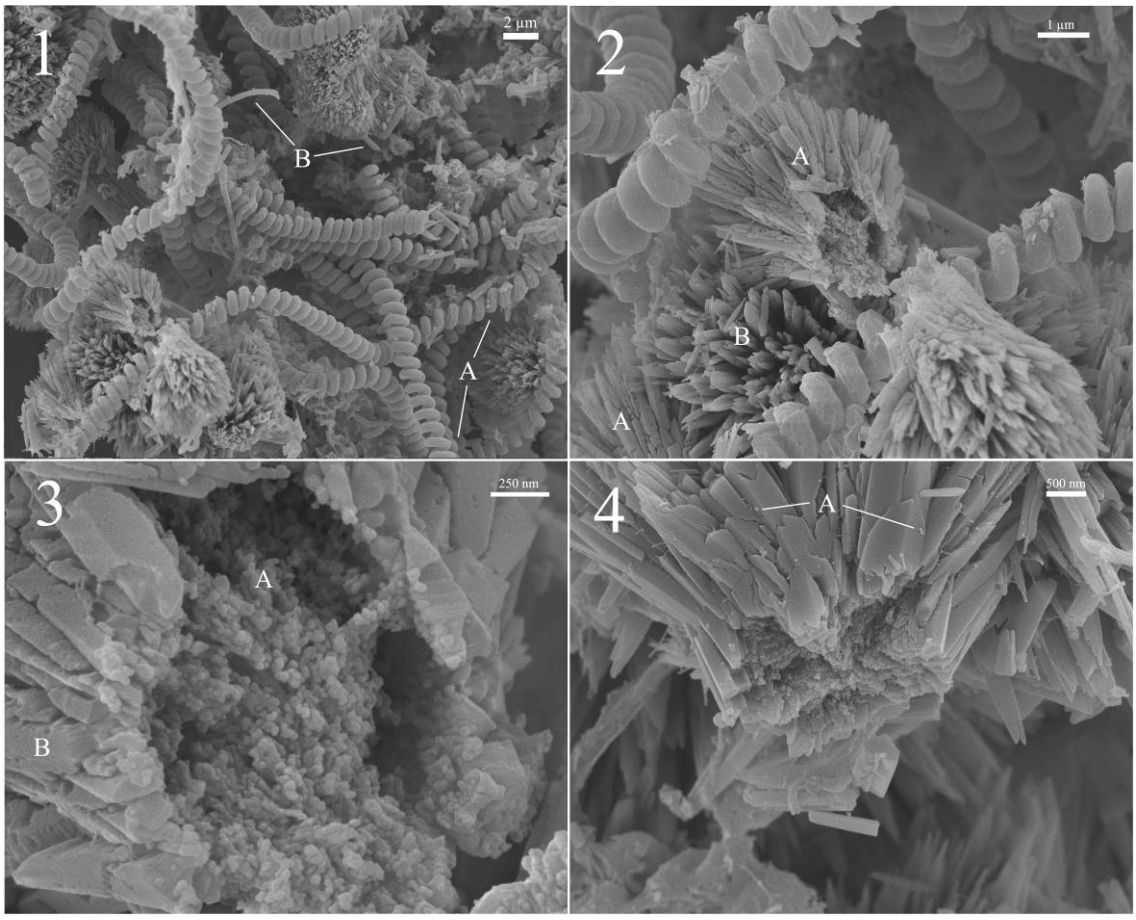

Figure 15 Acicular aragonite fuzzy dumbbells and associated microbes from Le Zitelle Springs, Viterbo, Italy. 1A: *Spirulina*; B: Rod-shaped microbes; 2A: Pitted aragonite crystals due to dissolution; B: Aragonite crystals free from dissolutional features; 3A: Amorphous ovoids within core; B: Pitted aragonite crystals at exterior; 4A: ~0.3 µm microbes on fuzzy dumbbell surface

At high magnification, *Spirulina* shows surface structures that may be artifacts, created when the sheath was desiccated; possibly, however, they may be features underlying the sheath (Figure 16.1). In areas where aragonite crystals are pitted (Figure 16.2A), new aragonite crystals have precipitated on the surface of *Spirulina* (Figure 16.2B).

www.manaraa.com

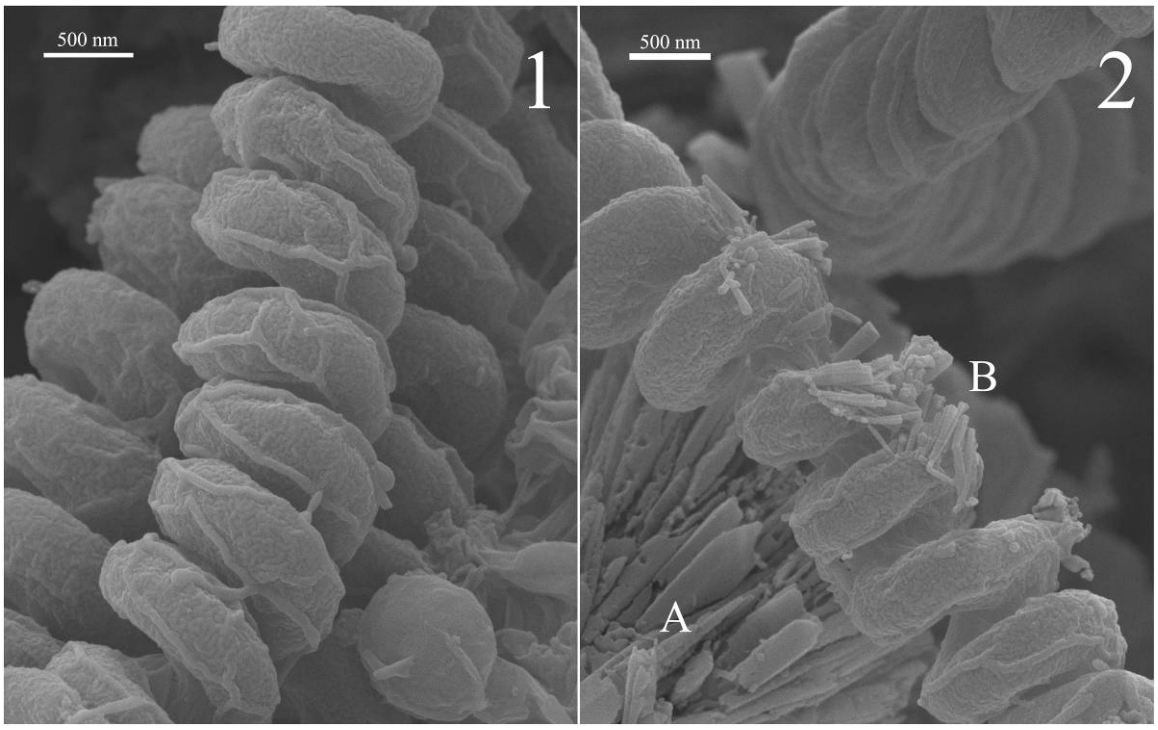

Figure 16 1: Surface features of *Spirulina*; 2A: Dissolution of acicular aragonite; B: Acicular aragonite precipitating on *Spirulina*

In a different part of sample 08D, a dumbbell is broken just at its "bar" (Figure 17.1 and 17.2). Crystals on this part of this dumbbell are more developed than those on other parts of broken dumbbells. The sub-micron filaments and sub-micron spheres seen elsewhere (Figure 1C and Figure 3F) are located here between the aragonite needles (Figure 17.1A). The spheres at the core of the broken surface show linear features radiating out from the core that align with crystal edges constituting the exterior of the dumbbell (Figure 17.2A). The heterogeneous spheres line up in chains extending towards the edge of the core (Figure 17.2B). These chains form elongate ovoids at a narrow ~200 nm transition zone between the core and the euhedral crystals.

www.manaraa.com

The lineations of heterogeneous spheres can be seen in sample 08D. They have the same "structure" as fuzzy dumbbells (core of spheres, thin transition zone, aragonite needle perimeter), but they do not have the same overall dumbbell shape (Figure 17.3 and 17.4). The aragonite needles, however, have angular euhedral terminals, not the rounded edges reported earlier. One obviously broken fragment of a needle shows a round edge at its terminus in figure 17.3A.

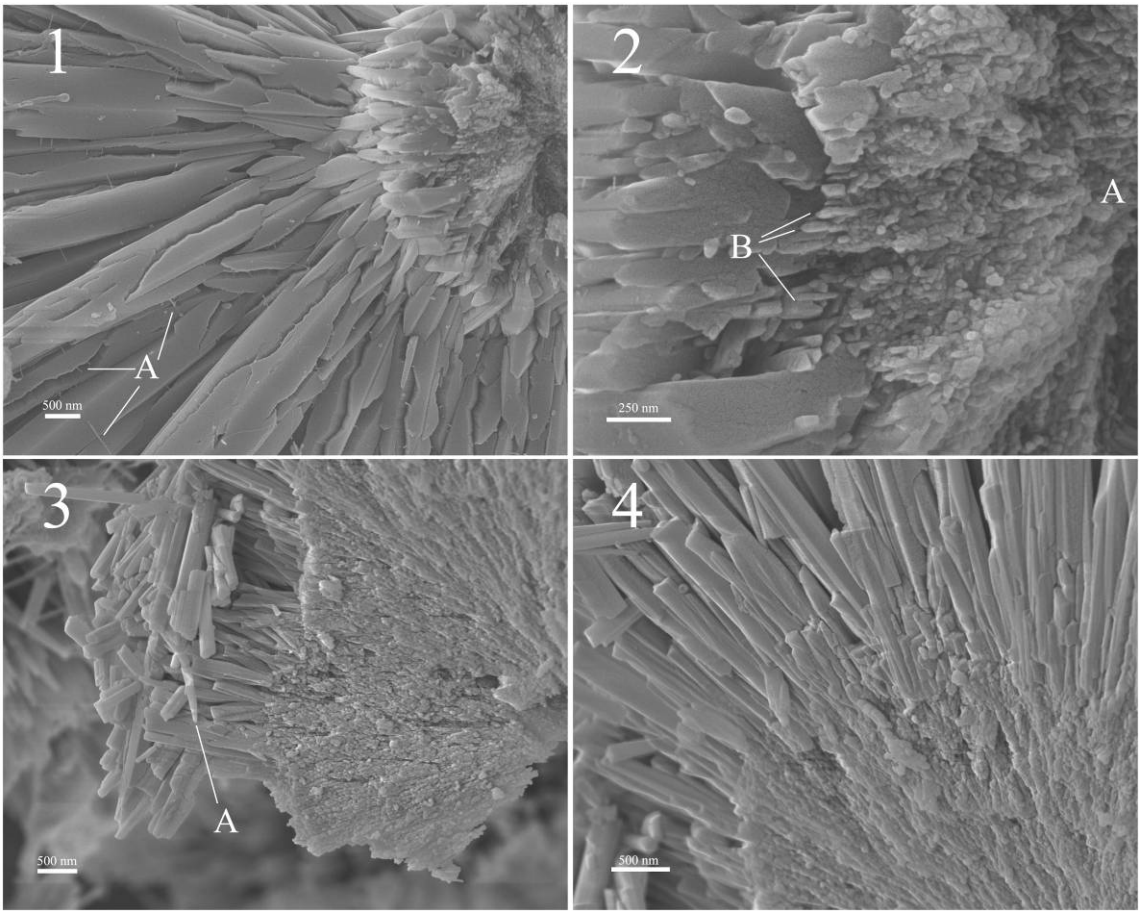

Figure 17 1A: Sub-micron filaments and sub-micron spheres on aragonitic fuzzy dumbbell; 2A: Amorphous heterogeneous core showing radial linear fabric; B: ~200 nm transition zone composed of elongate ovoids; 3A: Rounded terminus of broken aragonite crystal; 4: Similar features to those found in fuzzy dumbbells present within botryoidal acicular aragonite precipitate

www.manaraa.com

Transmission Electron Microscopy

Salt Pond Samples

Figure 18.1 shows a cross section of an aragonitic fuzzy dumbbell. *Spirulina* are present to right and left of the dumbbell. The core of the dumbbell is heterogeneous with darkly stained patches and unstained patches. In figure 18.2 - a higher magnification image of the core of the dumbbell - the unstained patches are reminiscent of subhedral to euhedral protocrystals ($CaCO_3$ crystals in the earliest stages of formation). The center of the dumbbell is darker and has a linear trend parallel to the long axis of the dumbbell, suggesting that more organic material occurs in the core of the dumbbell with increasing mineralization on the margins. Figure 18.2 shows the margin of the organic-protocrystal interior and the transition to acicular aragonite crystals that form the "fuzzy" ends of the dumbbell. Figure 18.3 illustrates the transition zone at even higher magnification and shows elongate crystals inter-fingering with stained material. Though stained, this amorphous organic material is somewhat translucent where thin at the edges of the crystals. Figure 18.4 illustrates the same transition zone in cross section, and shows the gradient from the darkly stained center core, through the transition zone, to the aragonite crystals along the exterior margin of the dumbbell. These crystals are aligned parallel to the long axis of the dumbbell. In the center of the dumbbell, the acicular aragonite crystals are parallel to the transition zone from core to crystal, but at the fuzzy ends of the dumbbell, the acicular crystals are perpendicular to the transition zone from core to crystal.

www.manaraa.com

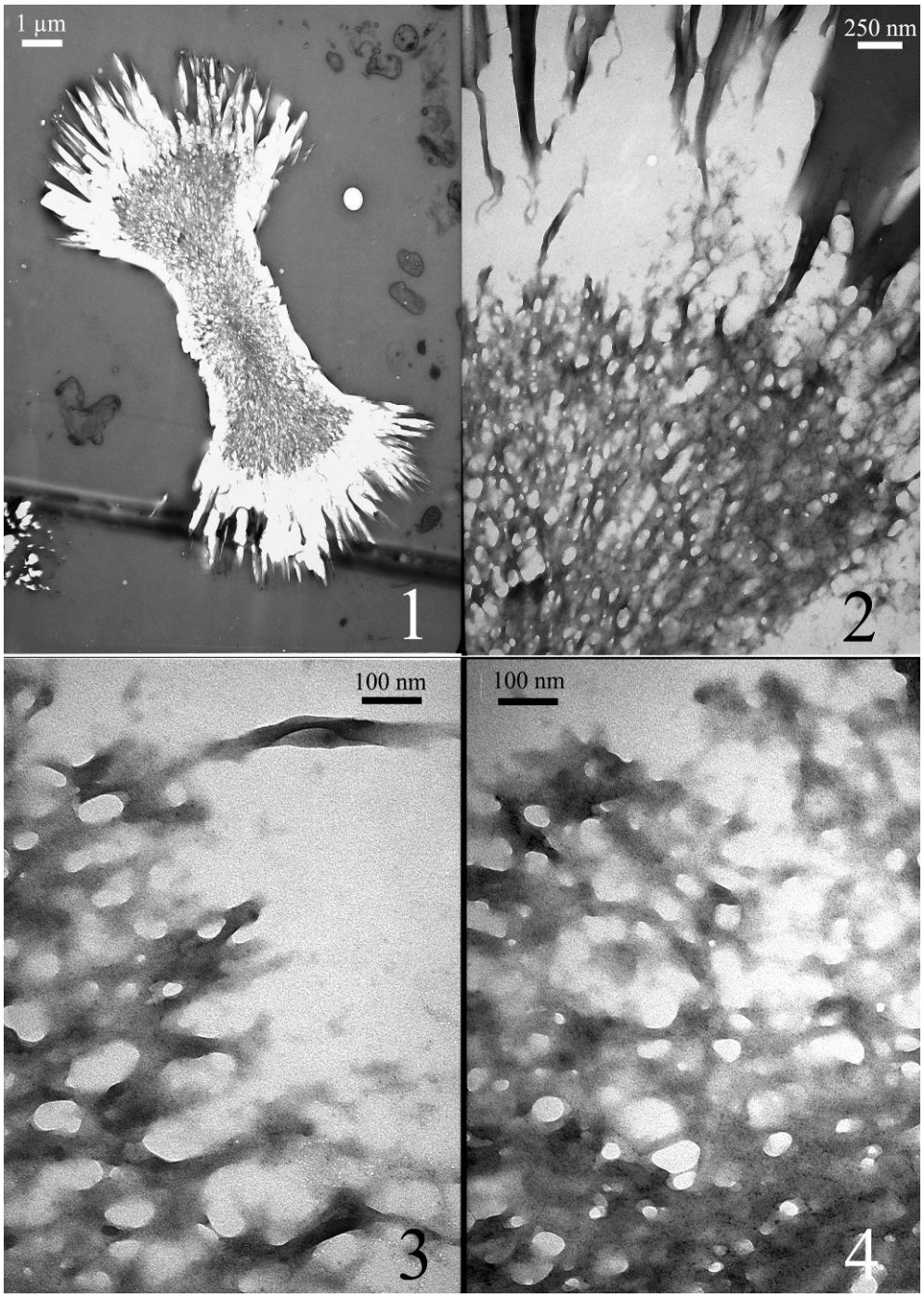

Figure 18 TEM images of an aragonitic fuzzy dumbbell in cross section. 1: 5000x image of entire dumbbell; 2: 20,000x image of fuzzy end of dumbbell; 3: 67,000x image of transition zone between organic and inorganic zones in "fuzzy" end of dumbbell; 4: 67,000x image of transition zone in "bar" region of dumbbell

www.manaraa.com

Figure 19 shows a fuzzy dumbbell, sections through *Spirulina* to the right and left, and other bacteria with cell walls. This dumbbell has a larger, darkly stained organic core and a thinner, aragonitic precipitate zone. The interior of the core parallel to the long axis is less darkly stained than the dumbbell described above (Figure 18). Once again, linear features are visible in the core of the dumbbell. In this example, as in the one described above, darkly stained core material surrounds unstained core material interpreted as subhedral to euhedral protocrystals. Figure 20.1 illustrates the elongated fabric of darkly stained material and the sharp boundary of the transition zone between the dark organic matter and the acicular aragonitic crystals, which are perpendicular to this ~200 nm transition zone. Figure 20.2 was taken at a magnification of 100,000X and shows the complexity of the stained interior core of the dumbbell. This complexity, caused by variations in shades of darkness within the dark zones, was not observable at lower magnifications. Once again, the transition zone is sharp with linear features interfingering at the boundary between exterior crystals and stained interiors. The evenly scattered small (~10 nm) dark spots on the crystal surface are interpreted as a precipitate formed during staining. The variations in darkness of the stained parts of the core are much more irregular than these "precipitate spots" and as such are interpreted to be the result of real variations in organic matter rather than an artifact of staining. Figure 20.3 was taken at 100,000X to illustrate the interior of the dumbbell, and shows amorphous organic matter, some as small patches within anhedral to subhedral protocrystals. The term "amorphous" is used because no distinct cellular-level structures are visible. The organic material appears irregular in shade and distribution. It is clumped together in round, elongate, and triangular patches of varying size, and staining pattern reveals

www.manaraa.com

varying shades of darkness, suggesting differences in density. Figure 20.4, taken at 140,000X shows anhedral to subhedral crystals fairly evenly distributed in an amorphous organic matter whose irregular staining pattern shows that it varies significantly in type and and/or density. The lighter patches may represent areas where the organic matter overlies a crystal in a different plane.

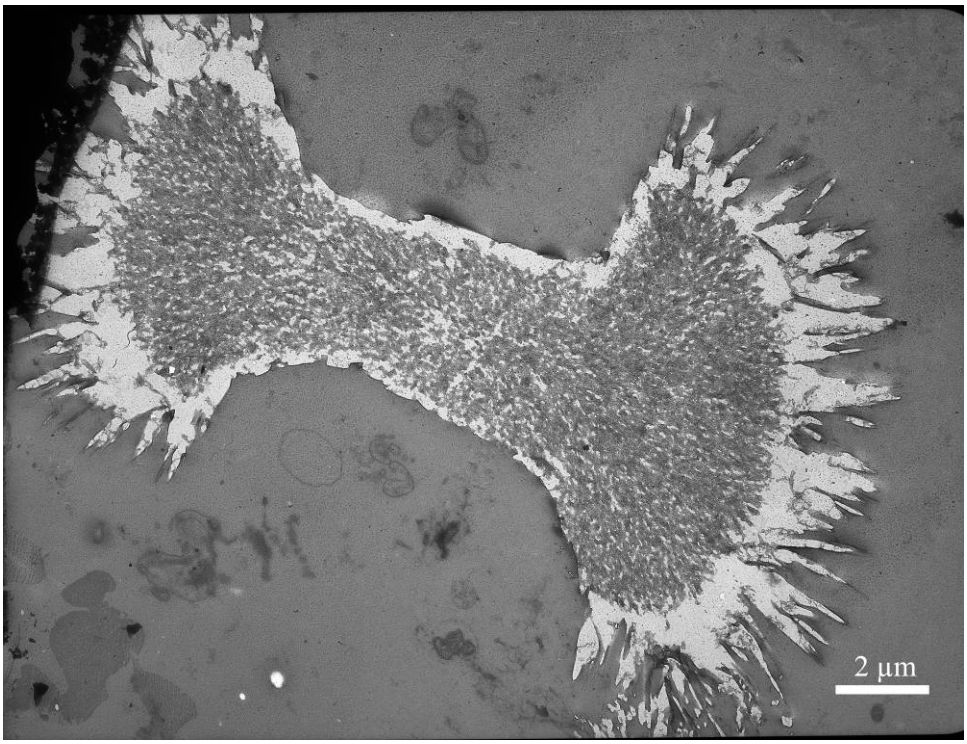

Figure 19 Aragonitic fuzzy dumbbell from Salt Pond, San Salvador, The Bahamas. Figure 20 shows areas of this dumbbell in greater detail

www.manaraa.com

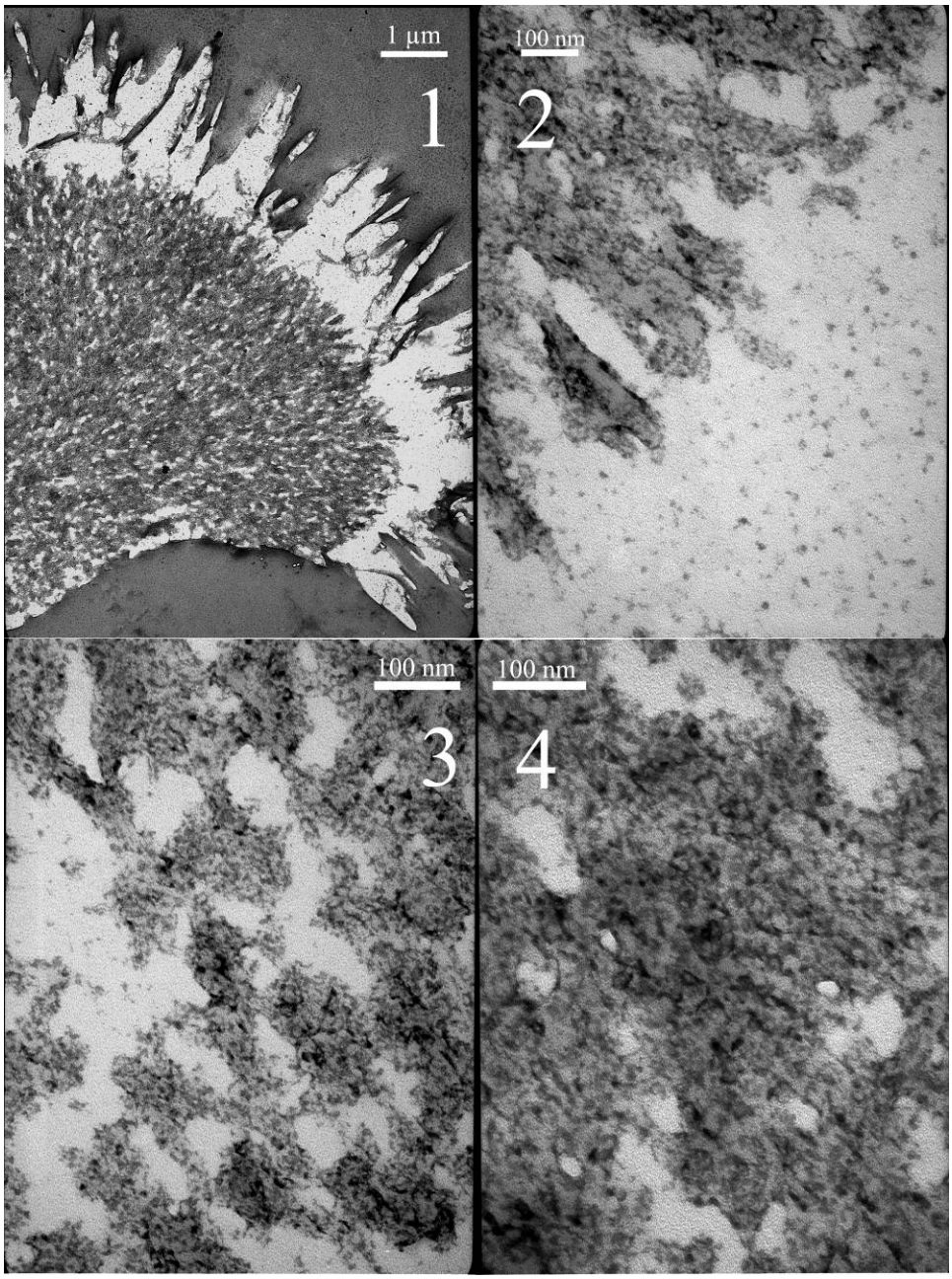

Figure 20 Details from Figure 19 at much higher resolutions. 1: 10,000x magnification of fuzzy end of dumbbell and ~200 nm transition zone. Radial linear features can be distinguished; 2: 100,000x magnification of ~200 nm transition zone; 3: 100,000x magnification of amorphous interior; 4: 140,000x magnifications – the maximum possible for the TEM at the MSU Electron Microscope Center in 2009

www.manaraa.com

Figure 21.1 taken at 4,000X shows the close association of a fuzzy dumbbell and a particularly dense population of *Spirulina*. The aragonite crystal itself shows no core, instead showing symmetrical zones (~1 µm thick) that are roughly perpendicular to the long axis of the dumbbell. At a higher magnification of 14,000X it is apparent that while most terminal ends of the acicular aragonite crystals at the "fuzzy" end of the dumbbell come to a fine point, a few show the same round morphology (Figure21.2) as seen in SEM samples 08C and 08D (Figures 9.B and 14.B).

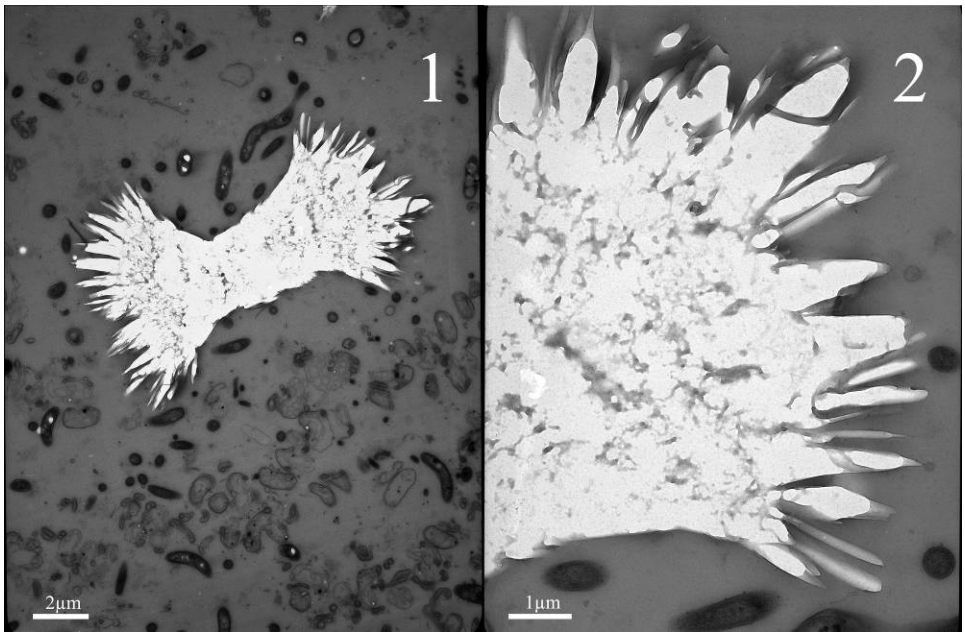

Figure 21 Aragonitic fuzzy dumbbell from Salt Pond, San Salvador, The Bahamas

Figure 22 shows a banded fuzzy dumbbell from Le Zitelle hot springs, Viterbo, Italy. The dumbbell is surrounded by biofilm with a linear fabric, a cross section of *Spirulina*, and possible nannobacteria. The dumbbell also has a darkly stained core, a

www.manaraa.com

clear and abrupt transition zone from core to crystal exterior, and approximately six layers of precipitate around the core. Based on previous studies of precipitate growth in this spring, these layers are interpreted to be daily growth bands.

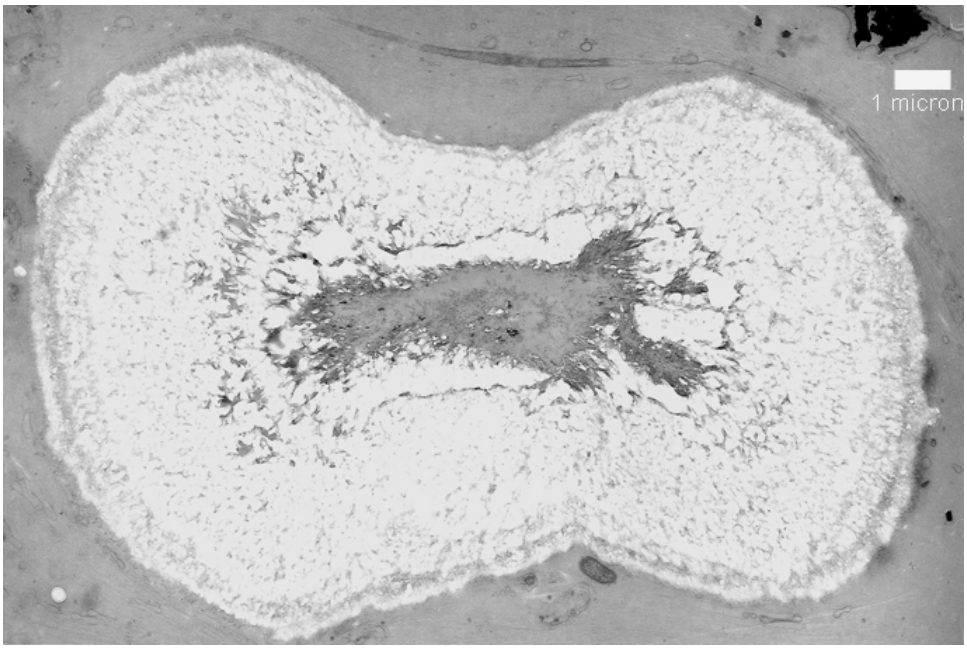

Figure 22 Aragonitic fuzzy dumbbell from Le Zitelle Springs, Viterbo, Italy. Photomicrograph by Dr. B.L. Kirkland

Figure 23.1 taken at 8,000X illustrates the finest cross section slice through *Spirulina* obtained and a nearby fuzzy dumbbell. Figure 23.2 shows another fine cross section of *Spirulina* in a different orientation. Images such as these greatly aid identification of *Spirulina* in less ideal cases.

www.manaraa.com

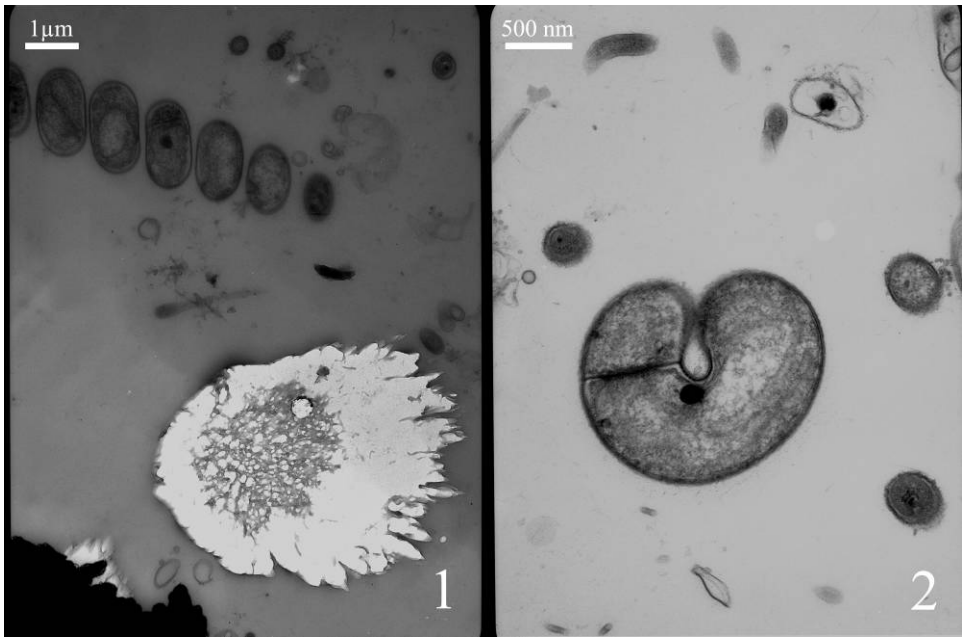

Figure 23 1: 8000x image of aragonitic fuzzy dumbbell from Salt Pond, San Salvador, The Bahamas, with typical associated *Spirulina*; 2: 20,000x image of a cross section through *Spirulina*

Reef Samples

SEM and TEM photomicrographs from reef samples showed no calcium carbonate precipitates. The following figures are typical of the unidentified biota observed.

Figure 24 is a composite image made from two photomicrographs which illustrates the linear fabric of a reef biofilm, and was common in samples from the reef. Figure 25 shows an unidentified cell common in all reef samples. Figure 26.1 illustrates crystal growth within a cell. This type of cell with some degree of internal crystal formation was present in all reef samples. Figure 26.2 shows clearly at higher magnification the euhedral nature of these crystals. Figure 27.1 shows that the darkly stained precipitates in this photomicrograph have a similar shape to the core of our fuzzy

www.manaraa.com

dumbbells. Figure 27.2 at a higher magnification of 20,000X illustrates the dark elongate shape. The precipitate appears to be "floating" on the image. The ovoid precipitate is interpreted as an artifact of staining based on the appearance of being "on" and not "in" the cut section (personal communication 2009, Amanda M. Lawrence).

www.manaraa.com

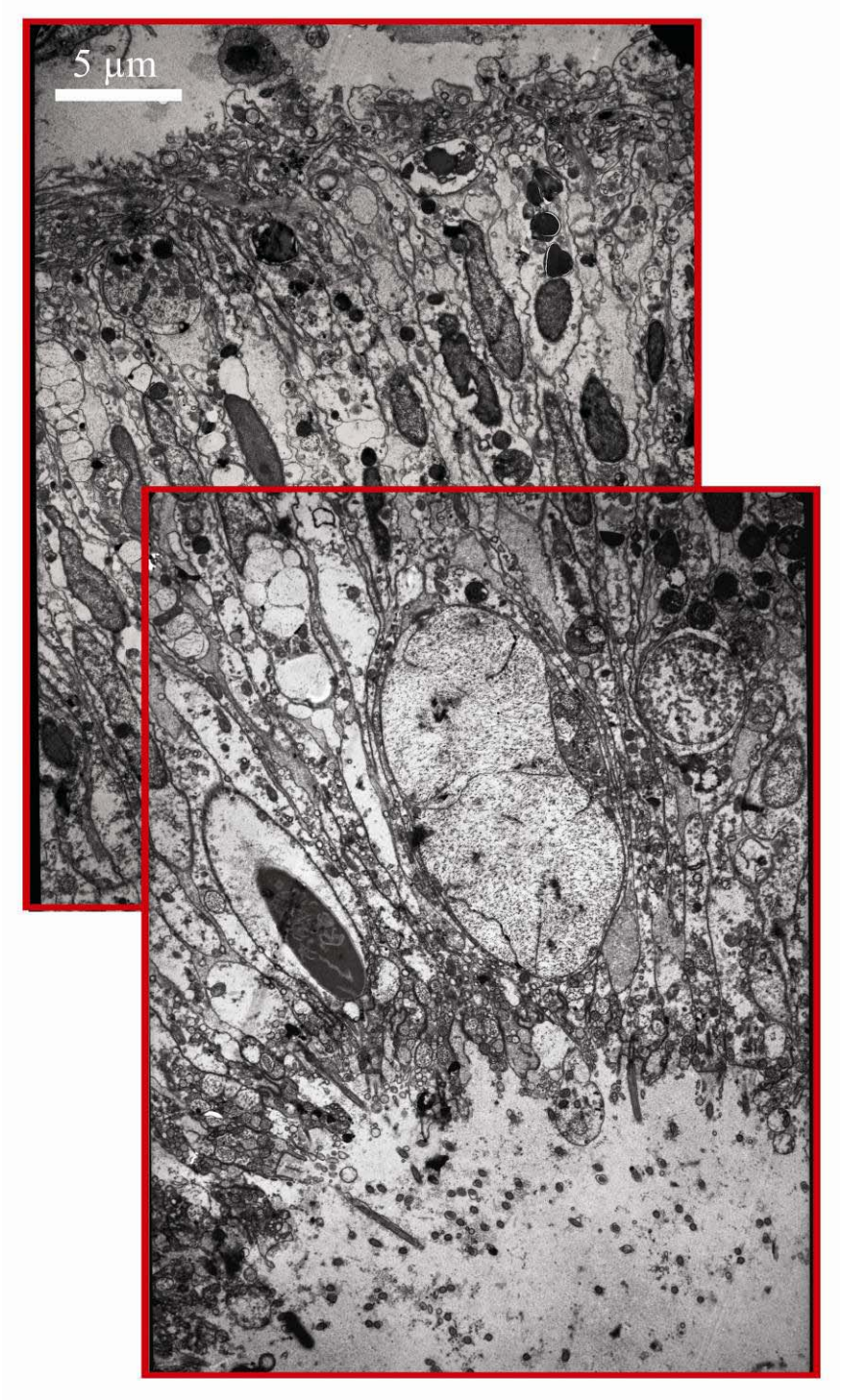

Figure 24 A typical fabric in reef biofilm from Fowl Cay Reef, Abaco, The Bahamas

www.manaraa.com

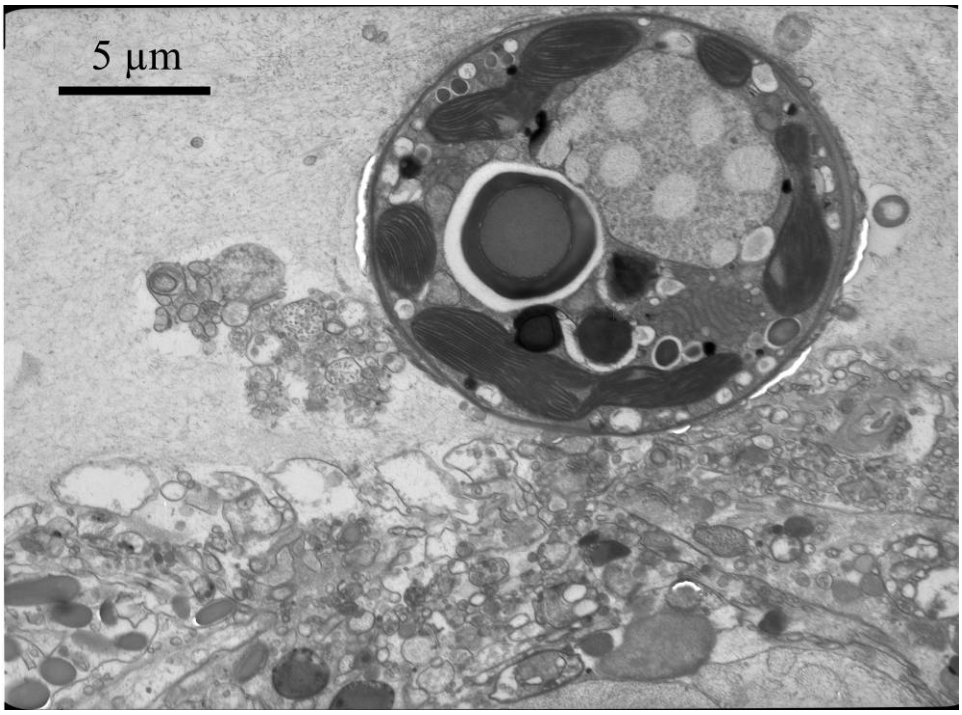

Figure 25 An unidentified cell common in biofilms from Fowl Cay Reef, Abaco, The Bahamas

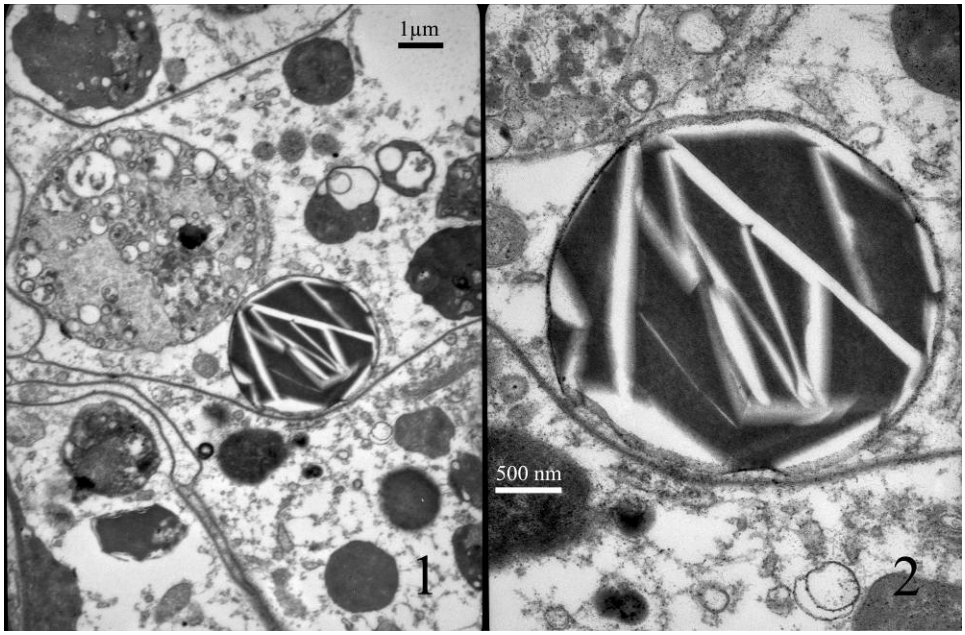

Figure 26 Crystal growth within a cell commonly found in biofilms from Fowl Cay Reef, Abaco, The Bahamas

www.manaraa.com

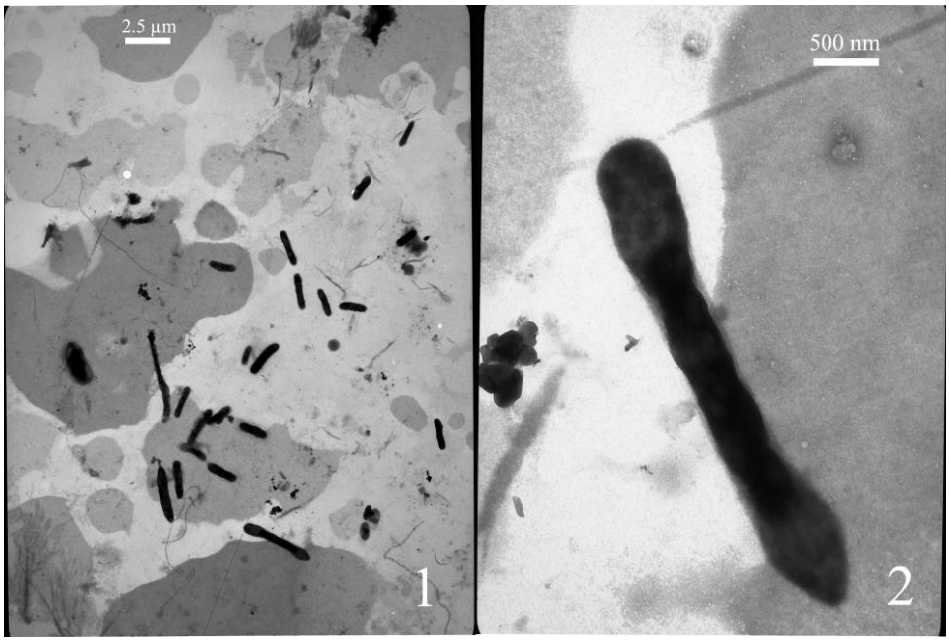

Figure 27 1: shows a collection of elongate ovoid precipitates, ~1-2 µm in length. 2: At 20,000x the slight dumbbell shape is more clearly seen. These precipitates do not have the same core features as aragonitic fuzzy dumbbells and are interpreted as artifacts of the staining process

Other Approaches

Photomicrographs from other types of microscopy can be used to clearly identify inorganic precipitates in close association with organic matter. Confocal and atomic force microscopy yield colorful dynamic images useful for initial analysis of samples. Both of these techniques are limited in resolution and cannot reveal the fine core structure in fuzzy dumbbells. ESEM is useful to show the relationship between inorganic precipitates and unprocessed biofilms that surround them, however images created with ESEM did not prove as useful in this study for addressing the question of the role of organic matter in the initial stages of precipitation. SEM analysis is ideal for creation of high magnification images, but is not useful in drawing a distinction between amorphous

www.manaraa.com

organic and amorphous inorganic matter. TEM was most useful in distinguishing, at very high resolution, the difference in amorphous features of the fuzzy dumbbell core.

www.manaraa.com

CHAPTER VI

DISCUSSION

The FESEM and TEM images presented in this study show that precipitation does occur in biofilms and more specifically, fuzzy dumbbells initiate on organic matter within biofilms. *Spirulina*-dominated biofilm appears to create the same microenvironment in salt ponds and hot springs, suggesting that in creating microenvironments for $CaCO_3$ precipitation, microbes play a stronger role than first suspected. Gothic calcite and fuzzy dumbbells were found in the hot springs, and fuzzy dumbbells were found in the salt pond. Hot spring and salt pond environments are geographically and chemically distinct, yet they contain similar features. Calcium carbonate precipitates were found in the reef samples, and it is suspected that the microenvironment in the reef biofilm was different, firstly because the microbes that dominate it were different, and secondly because it existed in normal marine sea water. To find precipitates in the reef environment, it may be necessary to obtain thicker or older biofilms from deeper in the reef wall. It is possible that precipitation in the reef requires more time and greater flux due to the relatively low concentration of minerals in seawater as compared to hot spring or salt pond locations (Moore, 1989).

In hot springs and salt pond microbial mats at the millimeter- and micron-scale microenvironments seem to control the initial stages of precipitation and sometimes dissolution. Strong evidence for the microenvironments is pitting on crystal surfaces

www.manaraa.com

from sample 08D (Figure 15.2 and 15.3), which is interpreted to be localized dissolution of aragonite. Other evidence from this sample suggests that microenvironments promote precipitation (Figure 16.2). For example, acicular aragonite crystals are clearly precipitated on *Spirulina* near a pitted aragonite dumbbell. Other fuzzy dumbbells of aragonite in this sample do not, however, show dissolution or reprecipitation.

Even stronger evidence for the microenvironments is found in Bullicame Dante Springs and Bullicame Piccolo Springs. Here the spring waters, supersaturated with respect to calcium carbonate, have a temperature in the range of 50 to 58°C. The conditions dictate that primarily aragonite precipitation should dominate (Folk, 1994), however, within biofilms, calcite is the dominant precipitate. In biofilms from the hot springs, calcite crystals seem to precipitate relatively slowly, and aragonite crystals precipitate relatively rapidly. Support for this interpretation is that organic filaments are caught in the calcite crystals while precipitation is occurring. In contrast, aragonite precipitating only microns away includes no organic filaments and shows no evidence (tubes or channels) of previous inclusion of filaments.

Evidence is found for the same microenvironments in microbial mats from Salt Pond, San Salvador, The Bahamas. Fuzzy dumbbells of aragonite occur in one part of one sample of the microbial mats. They were observed in serial ultramicrotome thin sections from which together encompass only a ~350 nm x ~250 µm x ~250 µm cubic section. Analysis of five samples from which over ~300 sections were made, showed that fuzzy dumbbells are usually absent. Fuzzy dumbbells are absent in all SEM and confocal samples from Salt Pond.

www.manaraa.com

Fuzzy dumbbells of aragonite are found from Salt Pond, The Bahamas and from Italian hot springs. Although these environments seem profoundly different, they do share common features. Of primary importance, both environments are supersaturated with respect to $CaCO_3$ (Chafetz and Folk, 1983). The hot springs are mineral-rich volcanic waters while ions in sea water in Salt Pond become concentrated by evaporation (during course of the study, salinities measured up to 80 ppt).

As an undergraduate research assistant in the W.W.Wilson lab group at the Mississippi State University Chemistry Department, I observed a tendency of supersaturated solutions to quickly form twinned crystals, in some cases (Figure 28), with dumbbell morphologies. This suggests that the fuzzy dumbbell morphology is the product of supersaturation, furthermore, it is possible that the morphology of proteins controls the intitial structure of calcium carbonate precipitates.

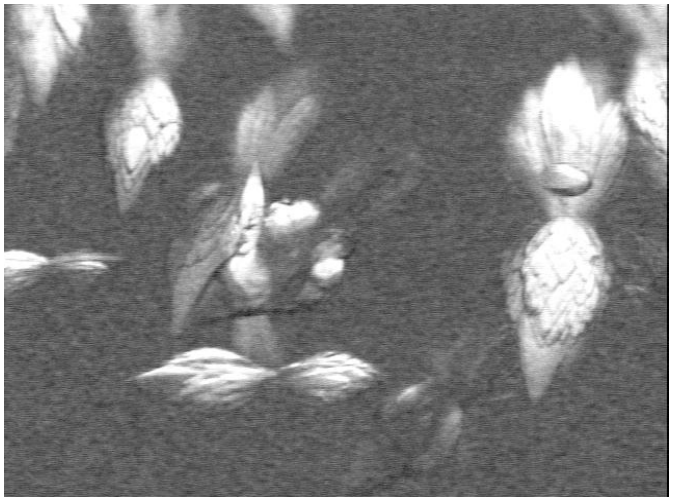

Figure 28 Equine serum albumin (a protein) crystals at 57X magnification grown from a supersaturated ESA solution.

www.manaraa.com

Another common feature of these disparate environments is the organism *Spirulina*, an extremophile cyanophyte. It is associated in both environments with the aragonitic fuzzy dumbbells. Microenvironments suitable for creation of fuzzy dumbbells also appear to be microenvironments in which *Spirulina* thrives.

Fuzzy dumbbells have long been noted from hot springs (Pursell, 1985) and tidal flats (Chafetz and Folk, 1983; Buczynski and Chafetz, 1992). Our research group, however, is believed to have the first TEM images of the core of fuzzy dumbbells (Dr. R.L.Folk, personal communication to B.L.Kirkland, October 22, 2008). TEM images are unique in that they reveal the fine scale (100,000X) features of the interior core of fuzzy dumbbells and record their initial stages of precipitation.

TEM images of the interior of these cores show amorphous organic matter, which is without visible cellular level structure, but that takes up organic stains. Although nannobacteria with distinctly visible cell walls are present in the biofilm in which we find fuzzy dumbbells (Figure 29), they are absent from the dumbbell core (Figure 20.4). Within the amorphous core are small subhedral unstained protocrystals. The amorphous core exhibits linear features that are parallel to the long axis of the dumbbell. It also shows a transition zone between the organic interior and the crystal exterior. The inner core is darker, which suggests that organic matter is dominant in the core and is a key to initial stages of calcite precipitation. The ~200 nm transition zone exhibits ovoid organic features that interfinger with ovoid features of the exterior aragonite crystals. The concentration of subhedral protocrystals of $CaCO_3$ increases from nearly absent at the predominantly organic inner core to abundant at the crystalline exterior. This gradation suggests that at the initial development of the dumbbell, amorphous organic matter is

www.manaraa.com

dominant, and that at some point in its early history inorganic precipitation becomes more dominant, eventually taking over and forming the outer crystalline sheath.

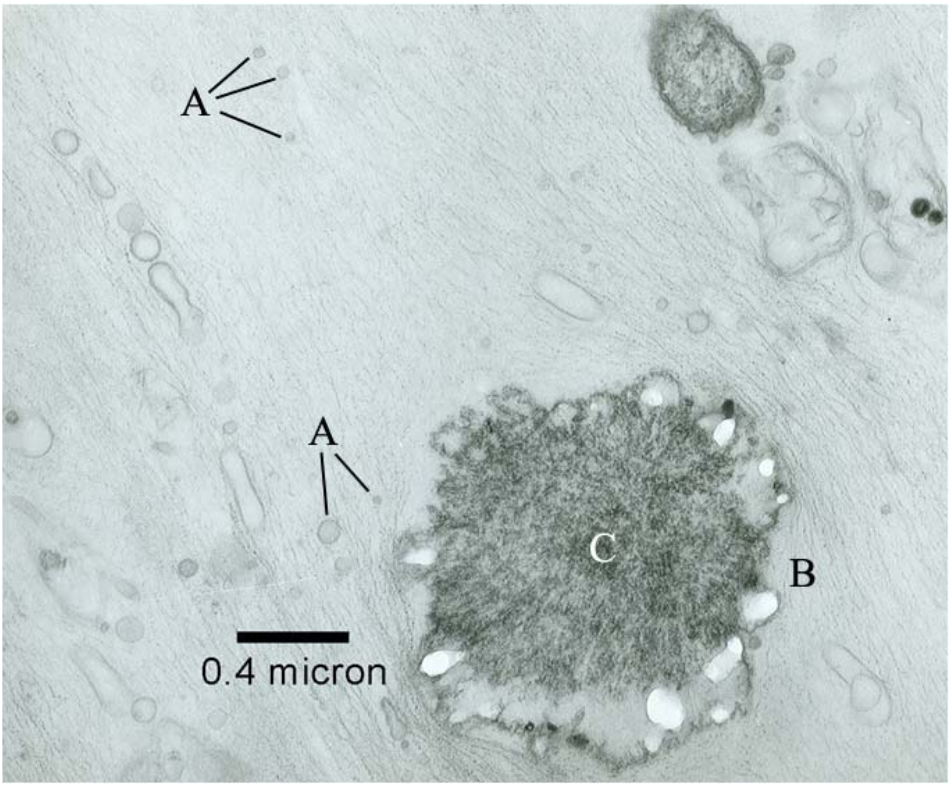

Figure 29 TEM image of biofilm from Le Zitelle Spring,Viterbo, Italy. A: Nannobacteria in linear fabric of biofilm; B: Incipient acicular aragonite, forming on amorphous core; C: Amorphous organic matter. Photomicrograph by Dr. B.L. Kirkland

SEM photomicrographs of core features show a similar phenomenon (Kirkland et al., 2008) however in these images, differences between amorphous organic material and subhedral protocrystals of $CaCO_3$ are not visible. Only a heterogeneous mass of ovoids, irregular in size and shape is observable (Kirkland et al., 1999). On freshly broken

www.manaraa.com

surfaces, these ovoids have a linear fabric radiating outward from the core (Figure 15.4A and Figure 17.2A) originating from the axis parallel to the long axis of the dumbbell. These linear, radiating features are analogous to those seen in TEM images. The ovoids form increasingly elongate shapes aligned perpendicular to the transition zone between amorphous core and crystalline exterior. Their size and placement are the same as that of the amorphous features in the transition zone seen in TEM (Figure 18.3). The transition zone is missing in the core of one broken dumbbell that shows pitting that is interpreted as dissolution of the surface of the crystals. Conceivably, the subhedral protocrystals are particularly sensitive to dissolution, and have preferentially dissolved the transition zone.

Multiple laboratory experiments show that nano-scale structures play a role in early precipitation and are associated with sulfate-reducing bacteria (Aloisi et al., 2006, Bontognali et al., 2008). These experiments describe, from samples prepared in the laboratory, phenomena that are similar to phenomena I have reported here from natural environments.

The original hypothesis that organic matter plays a key role in initial stages of precipitation in these environments is only truly testable at resolutions provided by TEM analysis. While confocal and ESEM analysis are useful for illustrating the juxtaposition of unprocessed biofilm and calcium carbonate precipitates, they proved inadequate for providing the high-resolution needed for observing the smallest structures of biofilms and precipitates. SEM analysis reveals fine-scale structures, but it is unable to distinguish with accuracy the difference in the core of dumbbells between amorphous organic and amorphous inorganic materials. With organic stains, TEM makes it possible to

www.manaraa.com

distinguish at 140,000X the fine structures of the transition zone and organic amorphous core from the subhedral protocrystals of $CaCO_3$ within the core of fuzzy dumbbells.

The significance of a study such as this may be far-reaching. An understaning of precipitation of carbonate in association with organic matter at the nanometer-scale, for example, may be applicable to medical studies such as microenvironments resulting in calcification in placentas (Agababov, 2003), arteries (Rasmussen et al., 2002), and kidneys (Kajander et. al, 1999). Understanding these phenomena is also potentially important in environments in which biofilm is present in supersaturated waters. Such environments span the gamut from Martian landscapes (McKay et al., 1997), to brines in oil reservoirs, to industrial applications, to purely academic ponderings.

www.manaraa.com

CHAPTER V

CONCLUSIONS

Calcium carbonate (aragonite) precipitation occurs within biofilms and on organic substrates within those biofilms in close association with bacteria in samples from Italian hot springs (aragonitic "fuzzy dumbbells" and two morphologies of calcite), and a Bahamian salt pond (aragonitic "fuzzy dumbbells"). Precipitates in these environments formed within biofilms.

Precipitation appears to occur in microenvironments based on evidence of specifically localized dissolution, reprecipitation, and the very localized occurrence of unique crystal morphologies. Microenvironments occur on the scale of millimeters in salt pond samples and microns in hot spring samples. In hot springs where the inorganic chemistry and temperature of the spring water would be conducive only to aragonite precipitation, calcite is precipitated within biofilms in the springs. Further evidence includes contemporaneous association of gothic calcite with growing organic filaments.

In both hot springs and salt ponds, fuzzy dumbbells contain a core of amorphous organic matter and subhedral microcrystals, which together exhibit linear fabric. *Spirulina* is consistently associated with dumbbells in both environments. Both environments are supersaturated with respect to calcium carbonate.

Confocal and ESEM were valuable for initial investigation into the association of organic matter and precipitates, however only FESEM and TEM were capable of

www.manaraa.com

providing the minimum 10,000X magnification necessary to adequately image the early stages and interior features of precipitation in these environments.

www.manaraa.com

REFERENCES

Agababov, R.M., Abashina, T.N., Suzina, N.E., Vainshtein, M.B., and Schwartsburd, P.M., 2007, Link between the early calcium deposition in placenta and nanobacterial-like infection: Journal of Bioscience, v. 32, p. 1163-1168.

Aloisi, G., Gloter, A., Krüger, M., Guyot, F., Zuddas, P., 2006, Nucleation of calcium carbonate on bacterial nanoglobules: Geology, v. 34, no. 12, p. 1017-1020.

Black, M., 1933, The algal sediments of Andros Island, Bahamas, Philosophical Transactions of the Royal Society of London, B 222, 165-192.

Bontognali, T. R.R., Vasconcelos, C., Warthmann, R.J., Dupraz, C., Bernasconi, S.M., and McKenzie, J.A., 2008, Microbes produce nanobacteria-like structures, avoiding cell entombment: Geology, v. 38, n. 8, p. 663-666.

Chafetz H.S. and Buczynski, C., 1990, Habit of bacterially induced precipitates of calcium carbonate and the influence of medium viscosity on mineralogy: Journal of Sedimentary Petrology, v. 61, no. 2, p. 226-233.

Buczynski, C. and Chafetz, H.S., 1992, Bacterially induced lithification of microbial mats: PALAIOS, v. 7, no. 3, p. 277-293.

Chafetz, H.S., 1986, Marine peloids; a product of bacterially induced precipitation of calcite: Journal of Sedimentary Research, v. 56, n. 6, p. 812-817.

Chafetz, H.S., and Folk, R.L., 1984, Travertines: depositional morphology and their bacterially constructed constituents: Journal of Sedimentary Petrography, v. 54, n.1 p. 289-316.

Dupraz, C., and Visscher, P., 2005, Microbial lithification in marine stromatolites and hypersaline mats: TRENDS in Microbiology, V. 13, n. 9, p. 429-438.

Flügel,E., Hillmer, G., and Scholz, J., 1993, Microbial carbonates and reefs: An introduction: Facies, v. 29, n. 1, p.1-2.

Folk, R.L., 1994, Interaction between bacteria, nannobacteria, and mineral precipitation in hot springs of central Italy: Geographie Physique et Quaternaire, v. 48, p. 233-246.

www.manaraa.com

Folk, R.L., personal communication to Corley, M.E., 22nd, October, 2008.

Folk, R.L., personal communication to Kirkland, B.L., 8th October, 2008.

Folk, R.L., personal communication to Kirkland, B.L., 22nd, October, 2008.

Gournay, J.P., Kirkland, B.L., Folk, R.L., and Lynch, F.L., 1999, Nanometer-scale features in dolomite from Pennsylvanian rocks, Paradox Basin, Utah: Sedimentary Geology, v. 126, p. 243-252.

Kajander, E.O., and Çiftçioglu, N., 1999, Nanobacteria: an alternative mechanism for pathogenic intra- and extra cellular calcification and stone formation: Proceedings of the National Academy ofSciences of the United States of America, V. 95, n. 14, p. 8274-8279.

Kirkland, B.L., Dickson, J.A.D., Wood, R.A., and Land, L.S., 1998, Microbialite and microstratigraphy; the origin of encrustations in the middle and upper Capitan Formation, Guadalupe Mountains, Texas and New Mexico, USA: Journal of Sedimentary Reearch, v. 68, n. 5, p. 956-969.

Kirkland, B.L., Lynch, F.L., Folk, R.L., Lawrence, A.M., and Corley, M.E., 2008, Nannobacteria, Organic Matter and Precipitation in Hot Springs, Viterbo, Italy: Distinctions and Relevance: Microscopy Today, v.16, n.6, p. 58-60.

Knoll, A. and Osborn, M.J., 1999, Size limits of very small micro-organisms: *in* Proceeding of a workshop, National Research Counsil, National Academy of Sciences, X, Washington D.C., pp. 148.

Lawrence, A. personal communication to Corley, M.E. January 15th, 2009.

McKay, D.S., Gibson, E.K., Thomas-Keprta, K.L., Romanek, C.S., 1997, Additional evidence for possible relic biogenic activity in Martian meteorite ALH84001: Geological Society of America, 1997 Annual Meeting, abstracts with programs, v.29, n.6, p.57.

McKay, D.S., Gibson, E.K., Thomas-Keprta, K.L., Vali, L.H., Romanek, C.S., Clemett, S.J., Chillier, Z.D.F., Maechling, C.R., and Zare, R.N., 1996, Search for past life on Mars: possible relic biogenic activity in Martian meteorite ALH84001: Science, v. 273, p. 924-926.

Miller, V.M. Rodgers, G., Charlesworth, J.A., Kirkland, B.L., Rodgers, J.C., Severson, S.R., Rasmussen, T..E., Yagubyan, M., Cockerill, F.R.III., Folk, R.L., Rzewuska-Lech, E., Kimar, V., Farell-Baril, G., and Lieske, J.C., 2004, Evidence of Nanobacterial-like structures in human calcified arteries and cardiac valves: American Journal of Physiology Heart and Circulatory Physiology, v. 287, p.1115-1124.

www.manaraa.com

Moore, C.H., 1989, Carbonate Diagenesis and Porosity: Amsterdam, Elsevier Publishing Company, pp. 338.

Nealson, K. H., 1997, The limits of life on Earth and searching for life on Mars: Journal of Geophysical Research, v.102, n.10, p. 675-686.

Pursell, V.J., 1985, The petrology and diagenesis of Pleistocene and recent travertines from Gardiner, Montana and Yellowstone National Park, Wyoming. pp. 154, The University of Texas at Austin, Austin, Texas.

Reitner, J., 1993, Modern cryptic microbialite/metazoan facies from Lizard Island (Great Barrier Reef, Australia) formation and concepts: Facies, v. 29, n. 1, p. 3-39

Riding, R., 2000, Microbial carbonated: the geological record of calcified bacterial-algal mats and biofilms: Sedimentology, v. 47, p. 179-214.

Shinn, E. A., Lloyd, R.M. and Ginsburg, R.N., 1969, Anatomy of a modern carbonate tidal flat, Andros Island, Bahamas, Journal of Sedimentary Petrology, v. 39, 1202-1228.

Spurr, A.R. , 1969, A low-viscosity epoxy resin embedding medium for electron microscopy: Journal of Ultrastructure Research, v. 26, p. 31-43.

Vasconcelos, C., McKenzie, J., 1997, Microbial mediation of modern dolomite precipitation and diagenesis under anoxic conditions (Lagoa Vermelha, Rio De aneiro, Brazil): Journal of Sedimentary Research, v. 67, n. 3, p. 378-390.

Zankl, H., 1993, The origin of High-Mg-Calcite microbialites in cryptic habitats of Caribbean coral reefs – Their dependence on light and turbulence: Facies, v. 29, n. 1, p. 55-59.

www.manaraa.com